National Advisory Committee
for Aeronautics
MAILED
FEB 28 1939
Library L.M.A.L.

TECHNICAL NOTES

NATIONAL ADVISORY COMMITTEE FOR AERONAUTICS

No. 675

THE CHARGING PROCESS

IN A HIGH-SPEED, SINGLE-CYLINDER, FOUR-STROKE ENGINE

By Blake Reynolds, Harry Schecter, and E. S. Taylor
Massachusetts Institute of Technology

Washington
February 1939

NASA Technical Library
3 1176 01425 6839

NATIONAL ADVISORY COMMITTEE FOR AERONAUTICS

TECHNICAL NOTE NO. 675

THE CHARGING PROCESS IN A HIGH-SPEED, SINGLE-CYLINDER, FOUR-STROKE ENGINE

By Blake Reynolds, Harry Schecter, and E. S. Taylor

SUMMARY

Experimental measurements and theoretical calculations have been made on an aircraft-type, single-cylinder engine, in order to determine the physical nature of the inlet process, especially at high piston speeds. The engine was run at speeds from 1,500 to 2,600 r.p.m. (mean piston speeds 1,370 to 2,380 feet per minute). Measurements were made of the cylinder pressure during the inlet stroke, and of the power output and volumetric efficiency. Measurements were also made, with the engine not running, to determine the resistance and mass of the air in the inlet-valve port at various crank angles.

A theoretical analysis of the process was made, on a purely mechanical basis (no account being taken of thermal effects). The results of this analysis indicate that, as far as the mechanics is concerned, mass has an appreciable effect but friction plays the major part in restricting flow.

From the pressure records it was found that the cylinder was filled to very nearly atmospheric pressure at bottom center, even at the highest speed. (Similar results were noted on a larger cylinder running at piston speeds up to 2,750 feet per minute.) The observed fact that the volumetric efficiency is considerably less than 100 percent is therefore attributed to thermal effects. An estimate was made of the magnitude of these effects in the present case, and their general nature discussed.

In connection with the analysis, it was necessary to obtain accurate records of the absolute cylinder pressure. Modifications of the M.I.T. indicator for this purpose are described in an appendix.

INTRODUCTION

The maximum power output of an engine is closely related to the quantity of air which it can pump. At high piston speeds, this quantity may be limited by the flow characteristics of the inlet valve. Previous experimenters, recognizing this limitation, have devoted considerable effort to determine the characteristics of steady flow (references 1, 2) and dynamic flow (references 3, 4, 5, 6) through valves. Work has also been done (references 3, 7, 8, 9) on the effect of inlet pipes of various lengths on the dynamics of air flow. This work has been largely devoted to engines operating at lower piston speeds, and information relating to the flow in the valve itself under actual operating conditions is incomplete.

The purpose of the present investigation is to establish the factors governing the flow of air* into the cylinder of an internal combustion engine operating at high piston speed, with particular attention to the relative importance of mass and friction in controlling the flow. It was expected that results of such a study might very well lead to a better understanding of the inlet process, if not to modifications of the conventional inlet arrangement for the purpose of increasing air capacity.

APPARATUS AND EXPERIMENTAL PROCEDURE

The engine used was an experimental Pratt and Whitney Wasp, jr. air-cooled aircraft engine cylinder mounted on a universal single-cylinder crankcase (fig. 1). (Dimensions are given in appendix I.) Cooling air was drawn (not blown) over the cylinder, to avoid the possibility of preheated air entering the inlet port.

Indicator diagrams were taken by means of an improved M.I.T. balanced-pressure indicator, using a Farnboro type cylinder unit developed especially for these tests. (See appendix II.)

During the tests the inlet pipe was removed, the fuel

---

*For convenience, the word "air" is used to denote the fuel-air mixture in the inlet system.

being injected directly into the inlet port by means of a nozzle located as shown in figure 1 and supplied from a special high-speed Bosch fuel-injection pump. Spark timing and fuel-air ratio were adjusted for best power conditions. The exhaust pipe was also removed during the tests, since it was found that the exhaust system caused considerable back pressure on the engine (see fig. 2).

Figure 3 shows a set of records of cylinder pressure, taken at various speeds from 1,500 to 2,600 r.p.m. These pressure curves are traced from light-spring indicator diagrams which were taken with a pointer speed of approximately 0.1 inch per second. The indicator contained S.A.E. No. 20 oil, and the corresponding error due to indicator piston friction is about 0.03 inch or 0.15 pound per square inch. (See appendix II, and figure 23.)

Quantities required for the theoretical analysis were determined as follows.

The natural frequency, $\omega_n/2\pi$, of the cylinder and valve acting as a Helmholtz resonator was determined at various points over the inlet stroke by exciting the resonator by means of a loudspeaker placed near the valve port and actuated by a calibrated beat-frequency oscillator (General Radio type 713-B). The results are accurate to within a few cycles per second, as resonance was quite sharp and easily discernible. Figure 4 shows the variation of the natural frequency with crank angle.

The effective valve area A defined as the area of an equivalent rounded-edge orifice, was determined from steady state flow data. The cylinder was evacuated to maintain a pressure drop across the intake valve and port of 12 inches of water by an exhauster connected to the exhaust port, the exhaust valve being held open. The quantity of air passed per unit time was measured by an air meter in the exhaust line. The meter was an N.A.C.A. Roots supercharger with a capacity of 0.180 cubic foot per revolution. Figure 5 shows the variation of the lift and of the effective area with crank angle.

Volumetric Efficiency

Volumetric efficiency e_v is herein defined as the

ratio of the mass of air taken in during one suction stroke, to the mass of air which would fill the piston displacement at inlet pressure and temperature.* For convenience in the discussion, the term "volumetric deficiency," defined as $(1 - e_v)$, will also be used.

Because of the difficulty of making a direct measurement of volumetric efficiency without disturbing the phenomena under investigation, it was decided to compute the volumetric efficiency from power measurements.

With the inlet pipe connected, the engine was operated at the same speeds as in the tests with no inlet pipe. A Nash "HyTor" compressor, which delivered air at approximately atmospheric temperature, was used to increase inlet pressure until the power was approximately the same as had been recorded with the inlet pipe off. From air measurements made by means of an N.A.C.A. Roots supercharger used as a meter, it was found that the volumetric efficiency was very nearly equal to 0.0058 (i.m.e.p.), where the i.m.e.p. was determined by adding the brake m.e.p. to the motoring friction m.e.p. The volumetric efficiencies used in this report are all computed from the above relation, and should be accurate to about 2 percent.

THEORETICAL ANALYSIS

According to the simplest view, the velocity of the air in the inlet valve is proportional to the piston velocity, the proportionality coefficient being the ratio of piston area to effective valve area. Such a view has been used in a previous investigation (reference 9), the results of which show that this gives a good approximation to the actual motion. A more careful examination requires that the impedance to flow at the valve be taken into account. Here the flow may be impeded by the inertia of the air in the valve, and by the friction encountered by the air in going through the valve.

For the purpose of analyzing the motion, the air in the valve is considered to move as a solid plug, of mass m. This plug is acted upon by three forces;

---

*For the experimental conditions used, inlet pressure and temperature are atmospheric.

F_1, the force due to the pressure outside the cylinder,

F_2, the force due to the pressure inside the cylinder,

F_3, the force due to the resistance to flow through the valve.

If u denotes the velocity of flow through the valve (measured positive for flow into the cylinder), the equation of motion is

$$\frac{d}{dt}(mu) = F_1 + F_2 + F_3 \tag{1}$$

the forces being measured positive in the direction of u.

The effective mass m may be found, approximately, from engine dimensions and the measurements described on page 3. The stiffness of the air in the cylinder is (reference 10, pp. 201-202).

$$k = \frac{\gamma P A^2}{V} \tag{2}$$

where γ is ratio of specific heats C_p/C_v

P, pressure in cylinder

A, effective valve area

V, volume of cylinder

The angular frequency of the free vibrations of the air in the valve is

$$\omega_n = \sqrt{k/m} \tag{3}$$

Thus m may be obtained from the relation $m = k/\omega_n^2$. The value of k is calculated from equation (2), using atmospheric γ and P since the frequency measurements were made at atmospheric conditions; and the value of ω_n^2 is obtained from figure 4. The resulting curve showing the variation of m with θ is given in figure 5.

The force due to the pressure outside the cylinder is simply

$$F_1 = AP_o \tag{4}$$

where P_o is atmospheric pressure.

The force due to the pressure inside the cylinder is

$$F_2 = -AP \tag{5}$$

In order to determine P it is assumed that the expansion of the air in the cylinder takes place isentropically. The relation between pressure and volume, for the cylinder contents at any instant, is then

$$\frac{dP}{P} = -\gamma\frac{dV - Audt}{V} \tag{6}$$

since the change in volume of the cylinder contents is $(dV-Audt)$ and the volume is V. Integrating, and solving for P,

$$P = P_o\left(\frac{V_2}{V}\right)^{\gamma} \epsilon \int_0^t (\gamma Au/V)dt \tag{7}$$

where P_o is initial pressure, assumed atmospheric,

V_2, initial volume, assumed equal to clearance volume

The force due to the resistance to flow through the valve may be approximated by

$$F_3 = -A(\Delta P) \tag{8}$$

where ΔP is the pressure difference (measured positive in direction of u) required to overcome the resistance and maintain steady flow of velocity u. For low velocities of flow this pressure drop is equal to $\frac{1}{2}\rho u^2$ (where

$T_i = \Delta T + \frac{1}{2}(T_w - T_e)$

ρ is the density of the air in the valve). Under actual running conditions, however, the velocity reaches quite large values, so that it is desirable to use the more exact expression. This expression may readily be derived if it is assumed that the expansion of the air from atmospheric conditions up to the conditions in the valve takes place isentropically and in accordance with the perfect-gas laws. The relation is (reference 11, p. 226)

$$\Delta P = P_o \left\{ 1 - \left(1 - \frac{\gamma - 1}{2\gamma} \frac{\rho_o}{P_o} u^2 \right)^{\frac{\gamma}{\gamma - 1}} \right\} \tag{9}$$

where ρ_o is atmospheric density.

For convenience, the equation of motion will be written in terms of a velocity <u>ratio</u> (instead of the velocity), namely

$$\beta \equiv u/c \tag{10}$$

where

$$c^2 \equiv \gamma P_o/\rho_o \tag{11}$$

Making appropriate substitutions, the equation of motion is obtained in the form

$$\frac{d\beta}{dt} = -\frac{1}{m}\frac{dm}{dt}\beta + \frac{AP_o}{mc}\left\{ \left(1 - \frac{\gamma-1}{2}\beta^2 \right)^{\frac{\gamma}{\gamma-1}} - \left(\frac{V_2}{V}\right)^{\gamma} \epsilon^{\int_0^t (\gamma Ac/V)\beta dt} \right\} \tag{12}$$

or

$$\frac{d\beta}{d\theta} = -M\beta + \frac{X}{\delta N}\left\{ 1 - Y - Z\,\epsilon^{\int_0^\theta (Q/\delta N)\beta d\theta} \right\} \tag{13}$$

where θ is crank angle (degrees A.T.C.)

N, engine speed (r.p.m.)

$M \equiv \frac{1}{m}\frac{dm}{d\theta}$

$$X \equiv AP_0/mc$$

$$Y \equiv 1 - \left(1 - \frac{\gamma - 1}{2}\beta^2\right)^{\frac{\gamma}{\gamma - 1}}$$

$$Z \equiv (V_a/V)^{\gamma}$$

$$Q \equiv \gamma Ac/V$$

The equation representing the motion is a nonlinear differential-integral equation with variable coefficients. Since the coefficients cannot readily be expressed analytically, it is practically impossible to solve the equation except by graphical-numerical methods. This can be done rather simply, since the equation gives the slope $(d\beta/d\theta)$ in terms of β and θ.

In order to solve the equation of motion (13), it is necessary to determine how the coefficients M, X, Z, and Q vary with θ. From the solution of the equation, the pressure in the cylinder may be obtained simply by using equation (7).

Determination of Coefficients

The coefficient M may readily be determined from m (e.g., graphically, by plotting log m against θ and measuring the slope of the resulting curve). The variation of M with θ is shown in figure 6.

The coefficient X may readily be obtained from the data in figure 5. The variation of X with θ is shown in figure 7.

The function Y may readily be calculated. A binomial expansion is convenient, three terms being sufficient (i.e., up to β^6). This function is plotted in figure 8, for three different values of γ.

The coefficient Z is readily obtained from engine dimensions; this coefficient is plotted in figure 9.

The coefficient Q, plotted in figure 10, is readily obtained from engine dimensions and the data in figure 5.

Careful examination reveals that the $M\beta$ term belongs in the equation of motion only when M is positive. When

M is positive the plug of air is picking up mass from rest, and the force which accelerates this mass is a part of the force acting on the plug, so that the $M\beta$ term must be retained in the equation. On the other hand, when M is negative, the mass lost by the plug is acted upon by a force, but this force is not a part of the force on the plug, and is irrelevant to the motion of the plug. Therefore when M is negative, the $M\beta$ term does not belong in the equation of motion.

A simplified analogy is the case of a moving train picking up or discharging bags of sand. If the moving train has bags thrown onto it (from rest), the train will be decelerated $(\dot{m} > 0, \quad m\dot{u} = -\dot{m}u)$; but if the moving train has bags thrown off it, the train will not be accelerated $(\dot{m} < 0, \quad m\dot{u} = 0)$.

The whole argument, of course, hinges on the supposition that the moving mass discarded by the plug (when $M < 0$) is brought to rest by external forces which act on the discarded mass without affecting the remaining mass (i.e., the plug). This will not always be true; e.g., if there is a sizable inlet pipe, the moving mass will be brought to rest partly by the containing walls adjacent to the valve, and partly by mixing with the air along the walls of the pipe; this latter part will affect the pressure acting on the plug. In such cases the effect is properly expressed by retaining some portion of the $M\beta$ term.

In the experimental work herein described, however, the inlet pipe was completely removed. Since the length of the port is only a few inches, the $M\beta$ term was omitted when $M < 0$.

Figure 11 (dotted line) is a pressure curve resulting from the solution of equation (13) for 2,600 r.p.m., with the experimental pressure record superimposed for comparison. It appears that the pressure is much too low except at the beginning of the suction stroke. This led to an investigation of nonmechanical effects on volumetric efficiency.

THERMAL EFFECTS

Examination of the experimental indicator diagrams revealed the rather astonishing fact that the <u>pressure at the time of inlet closing was nearly constant</u> over the range of

speeds investigated. In order to check this observation, the pressure P_θ was measured at a number of points along the early part of the compression stroke. From each of these pressures, an equivalent pressure at bottom center P_1 was obtained by means of the relation $P_\theta V_\theta^{1.35} = P_1 V_1^{1.35}$ where V_1 is the cylinder volume at bottom center and V_θ is the cylinder volume at the crank angle θ for which P_θ was measured. The values obtained by this method were consistent with each other, indicating that the exponent 1.35 was properly chosen for the cylinder contents at this time. The average of the equivalent P_1 is plotted in figure 12. (It should be noted that the actual pressure at bottom center is not P_1 since the inlet valve is still open and the flow is continuing after bottom center.) Results of this measurement show that P_1 is nearly 14.7 pounds per square inch and changes little over the speed range investigated. Further confirmation of this fact was found by noting that the compression lines of diagrams taken at various speeds appeared to be identical when superimposed. A series of three indicator diagrams taken from a Wright Cyclone engine with inlet pipe removed, at 1,600, 2,000, and 2,400 r.p.m. (piston speeds 1,830, 2,290, 2,750 feet per minute), showed a similar lack of variation in P_1.

The question immediately arises as to what causes the volumetric deficiency and what makes it vary with r.p.m. It is clear that the cause must be either an increase in temperature as the air comes into the cylinder, or a reduction of the partial pressure of fresh air in the cylinder due to dilution with fuel or residual exhaust gas.

Effect of Residual Gas

Part of the volumetric deficiency could be due to the effect of (1) the residual gas in the clearance space being at a pressure higher than atmospheric (2) the fact that the specific heat of the residual gas is somewhat different from that of the fresh charge, which will result in a different volume before and after mixing the two gases. These effects have been investigated (appendix III) and found to be negligible for the cases under consideration.

Effect of Fuel Evaporation

The addition of fuel also has an effect on volumetric efficiency. If no fuel evaporation occurs the effect is negligible. Evaporation causes a decrease in partial pressure of air and a decrease in the temperature of the mixture. The latter effect is much larger. Complete evaporation of fuel under adiabatic conditions and at the fuel-air ratio used (0.080) would cause a net volumetric deficiency of -0.04. (See reference 12.)

Effect of Throttling on the Temperature T_1

Assuming, for the moment, adiabatic conditions; as air flows through the inlet valve, the temperature will be reduced by expansion. The velocity it acquires during this process will, however, be completely converted into turbulent flow and eventually into random molecular motion. Assuming that the conversion of energy of turbulent flow to heat energy is completed immediately after entry into the cylinder, the temperature of the entering air will be the same as the outside temperature since air may be considered as a perfect gas for the pressures and temperatures under consideration (Joule-Thomson experiment). The air which has entered will then follow the pressure changes which occur in the cylinder and will eventually arrive at a temperature corresponding to isentropic compression from the entering pressure to the cylinder pressure at, say, bottom center. Thus, in general, each element of air will arrive at a different temperature, and since the pressure at bottom center is very nearly atmospheric, the temperature of most of the fresh charge in the cylinder will be above atmospheric. An estimate of the average temperature rise due to this process is possible if we take the piston work during the suction stroke equal to the heat energy causing the average rise in temperature.

The measured mean effective pressure during the suction stroke at 2,600 r.p.m. is 2.5 pounds per square inch below atmospheric and the work done is therefore 0.465 B.t.u. per cubic foot of inlet air. With an inlet-air density of 0.062 pound per cubic foot, 5 percent residual gas, and a mean specific heat of 0.24 B.t.u. per pound, the average temperature rise is $\frac{0.465}{0.062 \times 1.05 \times 0.24} = 30^\circ$ F. This will account for a volumetric deficiency of about 0.05. It is questionable how much of this effect is pres-

ent in the actual case since a considerable proportion of the energy of flow may not have been converted into random energy when the inlet valve closes.

Effect of Heat Transfer from the Cylinder Walls

There remains but one possible explanation for the observed volumetric deficiency: There must be a considerable transfer of heat to the charge, during the suction stroke, from the surfaces of the cylinder, inlet port, and valve. No data are available showing how much heat is transferred during flow through the port and valve and how much heat flows to the charge in the cylinder, nor is any experimental information available as to how the rate of heat flow varies during the cycle. It seems reasonable to suppose that the rate of heat flow from the inlet valve and valve seat to the flowing gas is comparatively large because of the high relative velocity and large temperature difference. At the beginning of the suction stroke the heat flow within the cylinder is undoubtedly in a direction from the gas to the cylinder wall, but as fresh charge comes in the temperature of the cylinder contents will be rapidly reduced and heat will flow in the opposite direction.

It should be noted that the effect of heat transfer may vary with speed and therefore be partly responsible for the variation in volumetric efficiency with speed. In addition to the fact that the nature of flow is changing, the temperature of the surfaces of the cylinder walls and particularly the temperature of the inlet valve may vary considerably with speed.

CORRECTION OF ANALYSIS TO ALLOW FOR THERMAL EFFECTS

An attempt was made to take account of the various thermal factors influencing flow. In order to accomplish this, it was necessary to find how much volumetric deficiency was due to effects other than a change in total pressure at the time of inlet closing. This was done by multiplying the observed volumetric efficiency by the observed ratio $14.7/P_1$. This quantity has been plotted in figure 12. At 2,600 r.p.m. the pressure is responsible for only a small volumetric deficiency and $14.7\ e_v/P_1 = 0.78$. Assuming that the flow of incoming air is adiabatic through

the valve and that immediately thereafter the net effect of heat transfer, fuel evaporation, and kinetic energy transfer is to raise its absolute temperature, thereby reducing its density by a constant factor, 0.78, the equation of motion is changed only in that the integral in equation (13) is divided by 0.78. The solid line in figure 11 is the pressure computed using this correction. The agreement with the experimental record is much improved, indicating that the above assumptions are reasonable.

Results of similar computations made for 2,200 and 1,500 r.p.m. are plotted, with the experimental records superimposed for comparison, in figures (13) and (14). The equivalent pressure P_1 obtained from the computed pressure at 198° crank angle, is plotted in figure 12. The difference between the computed and measured P_1 is approximately constant and equal to 0.3 pound per square inch. Apparently the analysis checks the variation of P_1 with speed over the range investigated. In this connection, it is interesting to note that the initial solution using no correction for thermal effects is approximately equivalent to an increase of 28 percent in r.p.m. and indicates a considerable reduction in P_1 at this higher speed (approximately 3,300 r.p.m.).

Previous investigators (references 3, 5) have assumed or concluded that the friction plays the major part in restricting the flow through the valve, the mass being relatively unimportant. In order to determine just how much the inertia does or does not affect the inlet process, the effect of omitting the mass from the foregoing analysis has been tried. With zero mass, the equation of motion becomes

$$1 - Y = Z\,\epsilon^{\int_0^{\theta} (Q/6N)\beta d\theta} \tag{14}$$

The resulting curve of pressure is plotted in figure 15 with the curve from figure 11 and the experimental record. It is evident that the analysis including mass fits the experimental data better, although the two solutions seem to be nearly identical during the latter part of the stroke. The nature of the difference between the curves suggests that an intermediate analysis, omitting the term $d\beta/d\theta$ but retaining the term $M\beta$, might be satisfactory.

CONCLUSIONS

The following conclusions have been drawn from the measurements and analysis:

1. Pressure drop in the valve is responsible for an extremely small part of the volumetric deficiency on the cylinder tested, even at 2,380 feet per minute mean piston speed.

2. The rise in temperature of the charge coming through the inlet valve and in the cylinder before inlet closing is responsible for a relatively large volumetric deficiency.

3. It is possible to calculate the pressure drop in the valve with good accuracy.

4. The friction of the air in the valve port is responsible for most of the pressure drop.

Recommendations

It is recommended that further study on this problem be directed particularly toward a study of the heat transfer process.

It also seems advisable to continue the work to still higher piston speeds. (This was not possible in the present investigation on account of the valve gear, which finally failed at 2,600 r.p.m.) The actual valve-lift curve should be observed since the valve lift when the engine is running at high speed may be considerably different from the lift measured statically at the same crank angle (reference 13).

Further improvement in the method of measuring pressures is desirable.

Massachusetts Institute of Technology,
Cambridge, Mass., June 1938.

REFERENCES

1. Tanaka, K.: Air Flow through Suction Valve of Conical Seat. Reports Nos. 50 and 51, Aero. Res. Inst., Tokyo Imp. Univ. (1929).

2. Hunter, D. U.: Effect of Port and Valve Shape on Air Flow through Intake Valves. S.B. Thesis, M.I.T. (1938).

3. Dennison, E. S.: Inertia Supercharging of Engine Cylinders. Trans. A.S.M.E. (1933), OGP-55-5, p. 53.

4. Aschenbrenner, J. A.: Der Einfluss der Gasträgheit auf den Liefergrad. Forschung auf dem Gebiete des Ingenieurwesens, vol. 8, Nov.-Dec., 1937, pp. 285-94.

5. Reynolds, B. G.: Dynamics of Air Flow through Intake Valve. S.M. Thesis, M.I.T. (1938).

6. Kemble, E. C.: Calculation of Low-Pressure Indicator Diagrams. T.R. No. 50, N.A.C.A., 1920.

7. List, Hans: Increasing the Volumetric Efficiency of Diesel Engines by Intake Pipes. T.M. No. 700, N.A.C.A., 1933.

8. Capetti, Antonio: Effect of Intake Pipe on the Volumetric Efficiency of an Internal Combustion Engine. T.M. No. 501, N.A.C.A., 1929.

9. Boden, R. H., and Schecter, H.: Dynamics of the Inlet System of a Four-Stroke Engine. (To be published) N.A.C.A. 3105-66

10. Morse, Philip McCord: Vibration and Sound. McGraw-Hill Book Co., New York, N. Y. (1936).

11. Prandtl, L., and Tietjens, O. G.: Fundamentals of Hydro- and Aeromechanics. McGraw-Hill Book Co. (1934).

12. Taylor, C. Fayette, and Taylor, Edward S.: The Internal Combustion Engine. International Textbook Co., Scranton, Penna. (1938).

13. Olmstead, E. H.: Study of the Dynamics of an Aircraft Engine Valve Gear. S.M. Thesis, M.I.T. (1938).

14. Taylor, E. S., and Draper, C. S.: A New High Speed Engine Indicator. Mech. Eng., vol. 55, Mar. 1933, pp. 169-71.

APPENDIX I

NOTATION AND NUMERICAL DATA

Notation

A, effective inlet valve area

c, velocity of sound, $\sqrt{\gamma P_o/\rho_o}$

e_v, volumetric efficiency

k, stiffness of air in cylinder

L, connecting-rod length

m, effective mass of air in the inlet valve

$M = \frac{1}{m}\frac{dm}{d\theta}$

N, engine speed, r.p.m.

P, pressure in cylinder during suction stroke

P_o, atmospheric pressure

P_1, equivalent pressure in cylinder at bottom center

P_θ, pressure in cylinder at θ during compression stroke

$Q = \gamma Ac/V$

r, crank radius

R, compression ratio

t, time

T, temperature

T_1, temperature of cylinder contents at bottom center

u, velocity of air in the inlet valve

V, volume of cylinder during suction stroke

V_1, volume of cylinder at bottom center

V_2, clearance volume

V_d, displacement volume

V_θ, volume of cylinder at θ during compression stroke

$X = AP_o/mc$

$$Y = 1 - \left(1 - \frac{\gamma - 1}{2}\beta^2\right)^{\frac{\gamma}{\gamma - 1}}$$

$Z = (V_2/V)^\gamma$

$\beta = u/c$

ϵ, base of natural logarithms

γ, ratio of specific heats, C_p/C_v

θ, crank angle, degrees A.T.C.

ρ, density of air in valve

ρ_o, atmospheric density

ω_n, natural frequency of air in valve and cylinder, $\sqrt{k/m}$

Physical Constants

$T_o = 530\ ^\circ R.$

$P_o = 14.7$ lb./sq. in.

γ: The average value of γ for the cylinder contents (air and residual gas) during the suction stroke has been taken as 1.3. For the charge at the end of the suction stroke 1.35 has been used.

$c = 1,130$ ft./sec.

Engine Dimensions

Bore	5-3/16 inches
Stroke	5-1/2 inches
$\frac{\text{Crank radius}}{\text{Connecting rod length}}$, $\frac{r}{L}$	0.234
Piston displacement, V_d	116.7 cu. in.
Compression ratio, R	6.5
Inlet-valve seat, inner diameter	2 inches

From the geometry,

$$V = \frac{V_d}{2}\left\{\frac{R+1}{R-1} - \cos\theta + \frac{L}{r}\left[1 - \sqrt{1 - \left(\frac{r}{L}\right)^2 \sin^2\theta}\right]\right\}$$

$$\simeq \frac{V_d}{2}\left\{\frac{R+1}{R-1} - \cos\theta + \frac{r}{2L}\sin^2\theta\right\}$$

APPENDIX II

M.I.T. BALANCED-PRESSURE INDICATOR

The indicator used to obtain pressure versus crank-angle diagrams of the cylinder was an improved M.I.T. type balanced-pressure indicator (reference 14), manufactured by the Otico Instrument Company (figs. 16, 21). The balanced-pressure principle upon which this indicator works is shown diagrammatically in figure 17. Typical light- and heavy-spring diagrams are shown in figures 18-20.

Since the determination of the small pressure drop across the inlet valve required an accurate record of the absolute pressure in the cylinder, greater precision was called for than had previously been accomplished. Therefore, considerable experimental work was done on the indicator in an attempt to increase its accuracy and determine its range of error.

As far as the indicator itself was concerned, it was found that somewhat greater accuracy could be realized for light-spring diagrams if the pressure pump was not in operation during the time that the diagram was being recorded, since the pressure fluctuations from the pump were enough to broaden the recorded line. Therefore, the pump was used only to drive the pointer to its maximum pressure position and was then shut off, the card being taken as the spark pointer returned to its atmospheric position. In taking heavy-spring diagrams, the width of the line is not increased perceptibly by the action of the pump, so that it is not necessary to use this lengthier procedure.

A second source of inaccuracy in the indicator itself arises from the speed at which the spark pointer is allowed to return to its atmospheric position. The indicator piston, spring, and oil-filled cylinder together constitute an overdamped vibratory system which has a definite time lag in following any forced motion. The constants of this system were determined by a simple experiment, as follows: The indicator drum was turned at a convenient speed, and the piston was moved away from its atmospheric position by hand, the bleed valve being open and the pump off. The "atmospheric" switch was then pressed and the piston released. The "atmospheric" switch of the Otico model (fig. 21) produces 120 sparks per second from the spark point to the drum so that the position of the pointer was recorded

every 120th of a second. The rotation of the drum spread the spark holes so that they could be easily identified and their distance from the starting position measured. A curve of displacement versus time (fig. 22) was then plotted, from which the time constant of the system was determined (equation (3), below).

As a forcing function a constant rate of change of balancing pressure was assumed. This assumption approximates fairly closely the actual operating conditions, where the bleed valve is opened continually wider as the balancing pressure decreases. From the assumed forcing function, the error was calculated as a function of the pointer speed and the spring constant. The error is expressed in inches displacement, on the diagram, from the position corresponding to the actual balancing pressure. Figure 23 is a plot of the error against the reciprocal of the speed of the spark pointer, for various springs with oil in the cylinder and for the 5-pound spring with and without oil. As may be seen, the removal of the oil raises the permissible speed considerably, in the case of light-spring recording.

The type of pick-up unit which had previously given the best results is one utilizing the motion of a clamped diaphragm (fig. 24) to make and break the grid circuit of the thyratron. The diaphragm, stamped from spring steel stock two- to five-thousandths inch thick, is supported on either side by perforated steel disks so that it will withstand a pressure somewhat more than 1,000 pounds per square inch. It was found by experimenting with several different designs that the nonadjustable contact-disk feature with a flat surface (fig. 24) makes for maximum ease of cleaning and reassembly without the need of readjustment. All of the required clearance for diaphragm motion is supplied in the front disk, which is cut down two-thousandths of an inch from a supporting rim at the edge. The back disk is flat. Approximately sixty holes, no. 55 drill, with no grooving, makes for good construction and operation without introducing any discernible error. The possibility of error arises from the fact that when the diaphragm is pressed against one of the disks the effective area may not be the same on both sides of the diaphragm. The possible effect of this unbalance, however, was not noticeable in a careful check between units with grooved and ungrooved disks. Therefore, it has been assumed negligible.

The chief disadvantage of the diaphragm-type pick-up

unit is that it is subject to a zero error, i.e., the entire indicator diagram is shifted up or down with respect to the atmospheric line. This error arises from the fact that the diaphragm generally has an initial pressure against the contact disk or against the front disk; a certain pressure is required on one side or the other in order to place the diaphragm in such a position that a slight change in pressure will make or break contact. The pressure required to place the diaphragm in this position is the zero error of the unit and is equal to the displacement of the diagram with respect to the atmospheric line.

In an attempt to measure the magnitude of the zero error so that corrections for it could be made, several means of calibration were devised. The simplest, an apparatus for static calibration (fig. 26), gives only a rough measure of the error, say to within a half inch of mercury. The shortcoming of the method lies apparently in the fact that the make and break occur much more slowly than under running conditions, a gradual change of resistance causing an indeterminate time of spark. As a means of increasing the rapidity of make and break, the fluctuations of the indicator pump can be utilized as follows. The unit is attached to the indicator in the usual manner except that the cylinder side of the diaphragm is exposed to atmospheric pressure. With the pump off and the bleed valve open, the drum is rotated and the atmospheric line recorded; this line will be in the correct position, corresponding to equal pressures on both sides of the unit. Then the bleed valve is closed and the balancing pressure slowly varied, until the unit interrupts the current and records an atmospheric line; this line will be in an incorrect position, corresponding to the pressures on the two sides of the unit differing by the zero error. Thus the difference in position between the two lines is the zero error of the unit. Because of the pressure fluctuations, the width of the atmospheric line recorded by a well-adjusted unit may be as much as 0.5 pound per square inch, but an average line drawn through this band was found to be in error by not more than 0.25 pound per square inch as compared with the reversal method of calibration.

Since neither of the foregoing methods simulates running conditions very closely, it was deemed wise to introduce another method, namely the reversal method, which would do so. One cylinder of an Indian motorcycle engine was redesigned with a two-to-one compression ratio head so that a complete indicator diagram could be obtained on a

scale sufficiently large to insure good accuracy. No valves were used, the pressure level being controlled by the flow of air into the cylinder through a small capillary tube. A critically damped manometer, although it did not read the average pressure in the cylinder correctly, nevertheless did serve as an excellent means of indicating whether the average pressure remained constant.

The method consisted of taking two diagrams on one card: one with the unit connected in the conventional manner and the other with the unit reversed end for end, i.e., the back side of the diaphragm, which is usually exposed to balancing pressure, was connected to the cylinder, while the front side was connected to the pressure line. Thus, whereas in one case the zero error would raise the diagram with respect to the atmospheric line, in the other case it would lower the diagram by the same amount. The resulting difference between the two diagrams is twice the zero error.

Since the flow of air in the unit is restricted by a small tube on the indicator side of the diaphragm, whereas there is no restriction on the cylinder side (fig. 24), it was necessary to design an adapter for the latter side, so as to make the assembly symmetrical about the diaphragm. The adapter, of course, introduced considerable lag in the transmission of pressure variations, so that true cylinder conditions were no longer present at the diaphragm. The indicator, however, records whatever variations are present at the diaphragm, and since these variations are unchanged by the reversal of a symmetrical assembly, the "forward" and "reverse" diagrams from the unit are congruent. The calibration is unaffected by the lag.

In practice it was found that the two diagrams were not exactly congruent due to the fact that the adapter did not make the unit quite symmetrical. Therefore, the zero error was taken to be half the difference between the average pressure lines of the two diagrams. A typical reversal calibration is shown in figure 27.

As these methods of calibration seemed to give fairly consistent results among themselves, it was decided to investigate the effect of temperature on the zero error. The results of the investigation proved conclusively that the diaphragm units under consideration were unsuitable for the measurement of absolute pressure to a greater accuracy than two pounds per square inch. The thought of accurate calibration of this type (i.e., the clamped-diaphragm type) was, therefore, abandoned.

As an alternative, the freely floating valve (Farnboro type) unit was resorted to (fig. 25). In order to obtain a clear-cut card from this type of unit it was found necessary to attach a fine wire between the valve and the center terminal; the contact between the valve stem and the necessarily loose guide was apparently poor enough to cause a broadening of the lines of the diagram. Even with this wire connection, however, the reversal method showed no zero error. It is reasonable to assume that a change of temperature will not introduce a zero error in this type of unit. This assumption is certainly justified by the consistency of the results obtained from this type of unit.

Another possible source of error is introduced with the valve unit, namely, a time lag due to the inertia of the valve. However, no perceptible lag was found, either from a careful check between diagrams taken with those and the diaphragm units, or from a study of the symmetry about the top-center line of a diagram from a nonfiring engine. The entire diagram was, of course, taken on "break" so that the time for the valve to cross the gap would not affect the recording.

The valve unit is, then, an excellent method of determining absolute pressures and as such can be used to determine the variation in the zero error of a diaphragm unit under operating conditions. The procedure is to superimpose diagrams taken by the two types of units under the same operating conditions. The true atmospheric line, determined from the diagram given by the valve unit, can then be drawn on the diagram from the diaphragm unit and the zero error measured off directly. By using this method over a range of operating conditions in the Wasp engine, it was found that the zero error of a diaphragm unit may change as much as 1.0 pound per square inch with a variation in speed from 1,500 to 2,600 r.p.m. A test previously run on a C.F.R. engine showed an increase in diaphragm temperature from 425° to 500° F. as the speed was increased from 900 to 1,800 r.p.m.; therefore, it is possible that the observed change in zero error is due to the effect of temperature.

A comparison of the results of the various methods of calibration is shown in table I. From these and other data it is safe to draw the following conclusions on calibration.

1) The static calibration - either hot or cold - of

a diaphragm unit that has been "run in" can be relied upon conservatively for an accuracy within 5 pounds per square inch - in most cases within 3 pounds per square inch.

2) Calibration with the indicator pump is comparable to static calibration.

3) The reversal method of calibration does not warrant the additional time required (i.e., not for routine calibration).

4) The valve unit needs no calibration, and can therefore be used to calibrate the diaphragm unit as mentioned above.

The effect of vibrations on the width of the recorded lines was studied in two ways. The C.F.R. engine with its heavy water-jacketed cylinder was considered substantially free of vibration, particularly when running at a low compression ratio. Diagrams taken from it, then, were assumed to be the best that could be obtained from the particular units which were used. In few cases did either the valve or diaphragm units give lines on the light-spring diagram which were wider than 0.3 pound per square inch, except during the exhaust stroke where it is doubtful whether the cycle repeats closely. The same units in the Wasp cylinder under the worst conditions of vibration gave lines sometimes as broad as 1.0 pound per square inch, but usually on the order of 0.7 pound per square inch. The valve units showed a tendency toward slightly broader lines than did the diaphragm type. Where lines broader than 1.0 pound per square inch were encountered, it was found that cleaning the unit would reduce the width to 0.7 pound per square inch, or less, for normal running conditions of the Wasp cylinder.

The second method of testing for the effect of vibration consisted of recording the make or break of contact of the unit when placed in a blind plug mounted in the cylinder wall. This shielded the unit from cylinder pressure but subjected it to vibration from the cylinder. With the engine running, the balancing pressure was slowly reduced to atmospheric. When the pressure was close to atmospheric in the case of the valve unit or close to the zero-error pressure in the case of the diaphragm unit, the motion of the vibrating cylinder head forced the unit away from the valve or diaphragm, the latter acting as seismic

masses. Thus contact was made or broken and a band was recorded on the diagram. These bands were compared with similar bands taken with the units stationary. Again the broadening effect of the vibration was found to be on the order of 0.5 pound per square inch.

The effect of vibration on the units, then, is merely to broaden the indicator lines. An average line drawn through the broader one is probably as accurate as the finer line from a nonvibrating engine.

TABLE I

INDICATOR UNIT CALIBRATION

All Pressures - Inches of Mercury

Unit No.	Diaphragm thickness (in.)	Static			Reversal	Running (against valve unit)
		Cold	Hot	Cold		
3	0.005	13	9	10	10.5	7.3
5	.002	11	11	12	12.3	9
7	.002	.5	.4	.5	1.0	.4
2	.005	+1.5	- .5	+1.5	+1.6	-4.0
6	.002	5	3	2	2.5	3.5

Unit No. 5, diaphragm 0.005 inch
Calibrated against valve unit in Wasp engine

r.p.m.	Inches Hg.
1,500	6.7
1,800	6.25
2,000	6.0
2,200	5.6
2,400	5.5
2,600	5.25

Unit No.	Static	Pump	Reversal
6	1.5	1.3	
6	1.7	1.4	
5		6.8	6.9
10	2.3		2.8
10		.8	.5
3	5.0		5.0
6		2.8	2.5
6	20	20.3	20.4

Calculation of Error Due to Pointer Speed

The error due to the pointer speed may be calculated by considering the response of the pointer to a forcing function.

The equation of motion is

$$m\ddot{x} + c\dot{x} + kx = kx_f \tag{1}$$

where x is pointer position

m, effective mass of pointer, spring, etc.

c, damping constant

k, spring constant

x_f, forcing function

Since the system is overdamped, equation (1) may be written in the approximate form

$$\dot{x} + \frac{1}{\tau} x = \frac{1}{\tau} x_f \tag{2}$$

where

$$\tau = c/k$$

The time constant, τ, may be determined from figure 22, which shows the measured response of the system upon being released from an initial deflection x_0. The complementary equation representing the free motion of the system is

$$\dot{x} + \frac{1}{\tau} x = 0$$

solving for $1/\tau$,

$$\frac{1}{\tau} = -\frac{\dot{x}}{x} = -\frac{1}{x}\frac{dx}{dt} = -\frac{d \ln x}{dt} \tag{3}$$

Thus $1/\tau$ is simply proportional to the slope of the straight portion of the response curve, figure 22.

With the time constant known, it is possible to find the error due to the lag in the response of the moving system to the varying balance pressure which acts as the driving force. As a close approximation to operating conditions, it is assumed that the pointer moves at a constant speed v. The forcing function is thus

$$x_f = vt \tag{4}$$

With this forcing function, the steady-state solution* of the equation of motion is

$$x = v(t - \tau) \tag{5}$$

The correct position of the pointer, corresponding to the actual value of the balancing pressure, is x_f (i.e., the position which the pointer would have if the system were purely stiffness-controlled; or, with the actual system, the position it would have if the motion were infinitely slow). The recorded position is x, given by equation (5). The error ϵ is defined as the correct position minus the recorded position,

$$\epsilon = x_f - x$$

From equations (4) and (5),

$$\epsilon = v\tau \tag{6}$$

The spring constant k is found** from the spring rating K (pounds per square inch per inch),

$$k = SK \tag{7}$$

where S is the area of the indicator piston.

*Since the time constant is of the order of 0.1 second, the complementary solution becomes negligible within about 0.5 second after motion starts.

**Or it can be measured directly, if necessary.

The damping constant c $(= k\tau)$ is presumably independent of the spring constant, and therefore may be determined by using any spring, knowing k and measuring τ as described above. Once this has been done, the value of τ for any other spring may readily be found from the relation $\tau = c/k$ by using the appropriate value of k.

From measurements made using the 5-pound spring, with S.A.E. No. 20 oil in the indicator cylinder, the error was found to be

$$\epsilon = 1.37 \frac{v}{K}$$

where ϵ is in inches, v in inches per second, and K in pounds per square inch per inch. A similar measurement, without oil, gave a result of $\epsilon = 0.11\ v$ for the 5-pound spring.

These results are plotted in figure 23.

APPENDIX III

CALCULATION OF THE EFFECT OF RESIDUAL EXHAUST GAS ON VOLUMETRIC EFFICIENCY

An estimation of the effect of residual exhaust gas on volumetric efficiency may be made for adiabatic conditions, that is, no heat flow to the walls of the container, and under the assumption that the residual exhaust gases are isentropically compressed or expanded to the same pressure as the inlet gases and then mixed.

The following symbols will be used:

P_0, atmospheric pressure

T_0, atmospheric temperature

P_1, pressure in cylinder at end of suction stroke (bottom center)

T_1, temperature of mixture at end of suction stroke

P_6, pressure in cylinder at end of exhaust stroke (top center)

T_6, temperature of residual gas at end of exhaust stroke

V_1, cylinder volume at end of suction stroke

V_2, clearance volume

$R = V_1/V_2$, compression ratio

n_a, number of mols of air in cylinder at end of suction stroke

n_r, number of mols of residual gas in cylinder at end of suction stroke

C_a, mean molal heat capacity of air (constant pressure)

C_r, mean molal heat capacity of residual gases (constant pressure)

γ, the ratio of specific heat at constant pressure to specific heat at constant volume, for residual gas at temperature T_6

R_0, universal gas constant

When the volumetric efficiency is unity, n_1, the number of mols of air taken in will be

$$n_1 = \frac{P_0(V_1 - V_2)}{R_0 \; T_0}$$

The volumetric efficiency e_v is therefore

$$e_v = \frac{n_a}{n_1} = \frac{n_a \, (R_0 T_0)}{P_0(V_1 - V_2)} \tag{1}$$

From the gas law,

$$P_6 \; V_2 = n_r \; R_0 \; T_6 \tag{2}$$

$$P_1 \; V_1 = (n_a + n_r) \; R_0 \; T_1 \tag{3}$$

If the residual gas is expanded or compressed isentropically to the pressure P_1 and the temperature T_7 and then mixed with the incoming charge,

$$T_7 = T_6 \left(\frac{P_6}{P_1} \right)^{\frac{1 - \gamma}{\gamma}} \tag{4}$$

The temperature of the mixture T_1 may be found from the relation

$$(T_1 - T_0)\ C_a\ n_a = (T_7 - T_1)\ C_r\ n_r$$

or

$$T_0 = T_1 - (T_7 - T_1)\ \frac{C_r\ n_r}{C_a\ n_a} \tag{5}$$

From (2) and (3),

$$\frac{n_a}{n_r} = R\ \frac{P_1 T_6}{P_6 T_1} - 1 \tag{6}$$

Combining (4), (5), and (6),

$$\frac{T_0}{T_1} = 1 - \frac{C_r}{C_a}\ \frac{\left(\frac{P_6}{P_1} \right)^{\frac{1}{\gamma}} - \frac{P_6 T_1}{P_1 T_6}}{R - \frac{P_6 T_1}{P_1 T_6}} \tag{7}$$

Combining (6) with (1) and (2),

$$e_v = \frac{P_1}{P_0}\ \frac{\frac{T_0}{T_1} \left(R - \frac{P_6 T_1}{P_1 T_6} \right)}{R - 1} \tag{8}$$

and substituting (7) in (8),

$$e_v = \frac{P_1}{P_o} \frac{R - \frac{C_r}{C_a}\left(\frac{P_6}{P_1}\right)^{\frac{1}{\gamma}} + \frac{P_6 T_1}{P_1 T_6}\left(\frac{C_r}{C_a} - 1\right)}{R - 1} \qquad (9)$$

It will be noted that one of the unknowns T_1 remains in the expression. However, T_6 is not altogether independent of T_1, and T_1/T_6 may be considered constant without appreciable loss of precision since T_1/T_6 is small, $(C_r/C_a - 1)$ is small, and the product is small compared to the other terms. The equation in this form is considerably simpler than it would be if T_1 were replaced by its value in terms of T_o.

Sample Computations

The ratio of the mean molal heat capacity of residual gas to that of air is approximately 1.1. For the temperature range investigated T_1/T_6 is approximately 0.3 and γ is about 1.31. Substituting these values in (9),

$$e_v = \frac{P_1}{P_o} \frac{R - 1.1(P_6/P_1)^{0.76} + 0.03(P_6/P_1)}{R - 1} \qquad (10)$$

or, for the engine used $(R = 6.5)$,

$$e_v = \frac{P_1}{P_o}\left[1.18 - 0.20(P_6/P_1)^{0.76} + 0.005(P_6/P_1)\right] \qquad (11)$$

In order to estimate the minimum effect of residual gas, the following values were determined from an indicator diagram, taken at 2,000 r.p.m., which showed a minimum value of P_6.

$$\frac{P_1}{P_o} = 1 \qquad \frac{P_6}{P_o} = \frac{P_6}{P_1} = 0.965$$

Substituting these values gives

$$e_v = 1.18 - 0.20\ (0.965)^{0.76} + 0.005$$

$$= 0.99$$

A second set of values was determined from an indicator diagram, taken at 1,500 r.p.m., which showed a maximum value of P_6.

$$\frac{P_1}{P_0} = 1 \qquad \frac{P_6}{P_0} = \frac{P_6}{P_1} = 1.027$$

The result of substitution of these values is

$$e_v = 0.985$$

It was concluded that the effect of residual gas could be neglected.

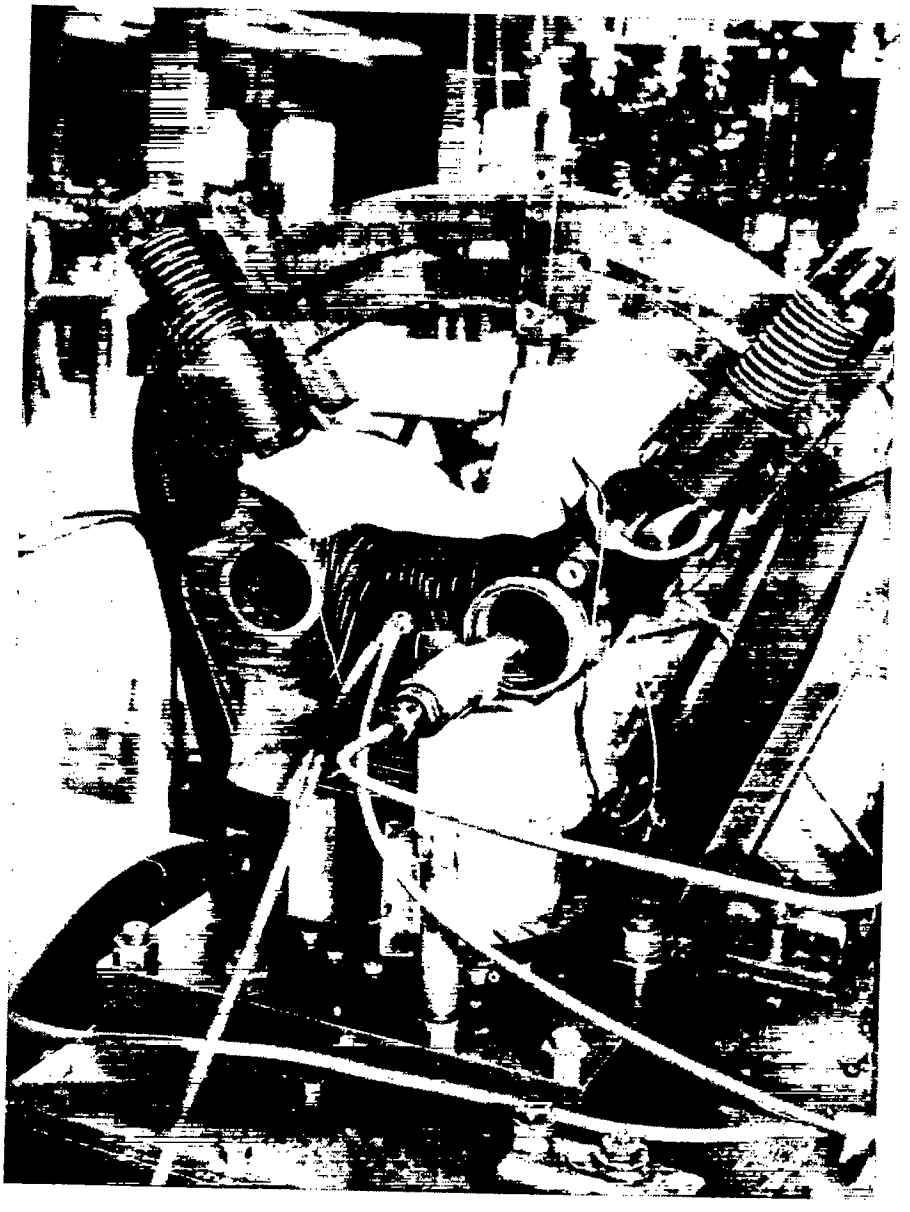

FIGURE 1.—WASP JR. CYLINDER ON UNIVERSAL CRANKCASE

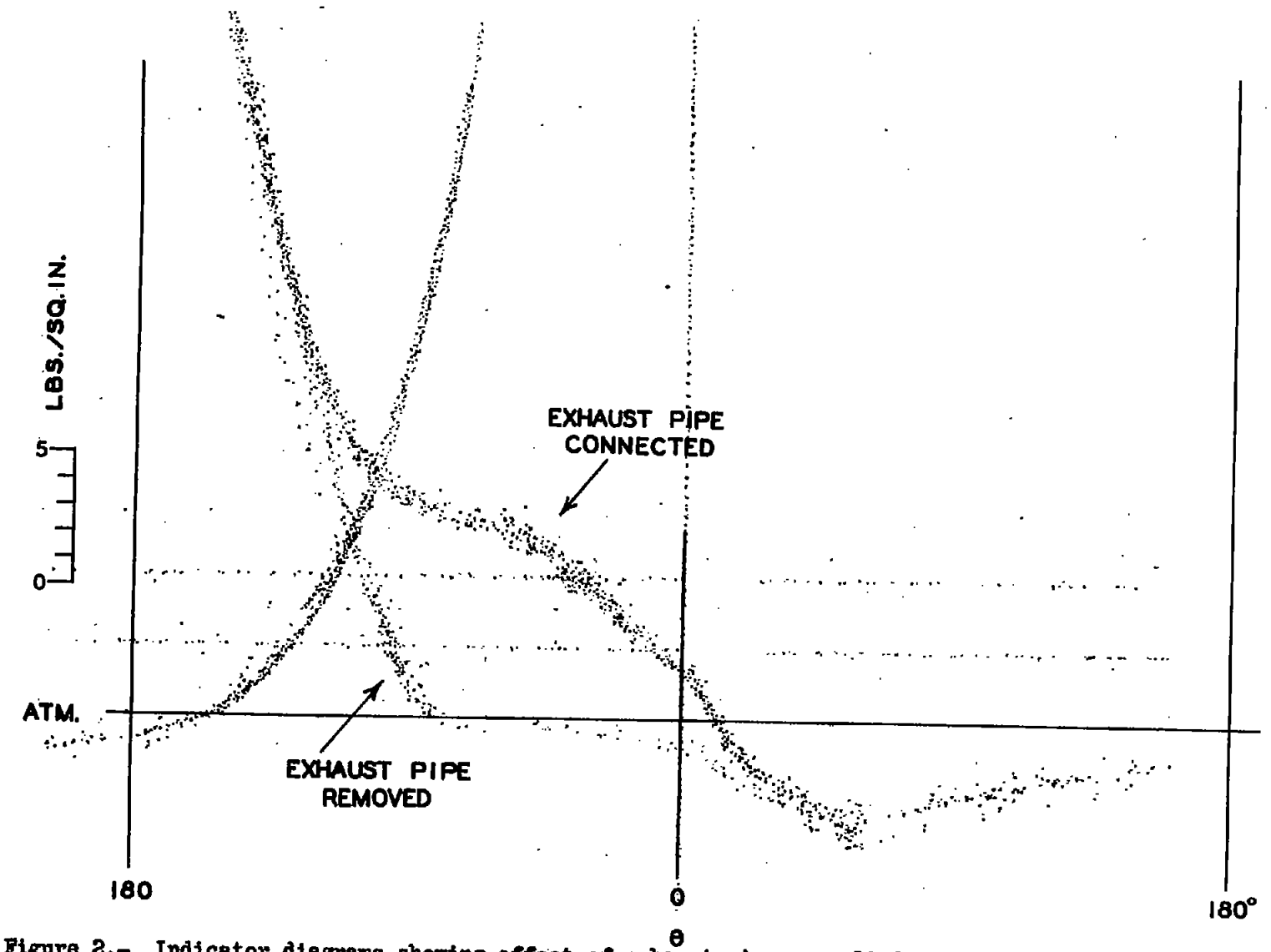

Figure 2.- Indicator diagrams showing effect of exhaust pipe on cylinder pressure. 2200 r.p.m.

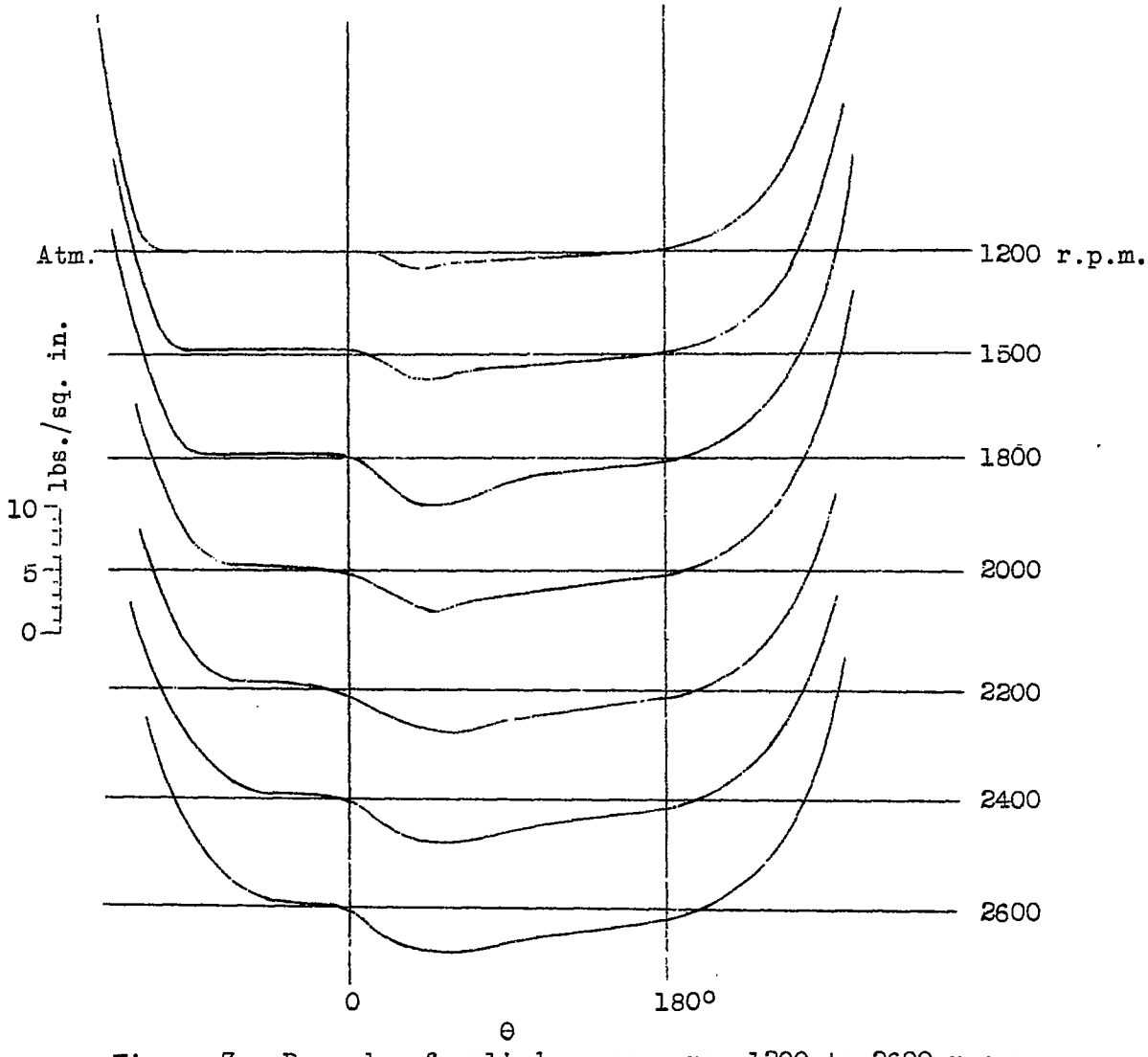

Figure 3.- Records of cylinder pressure. 1200 to 2600 r.p.m.

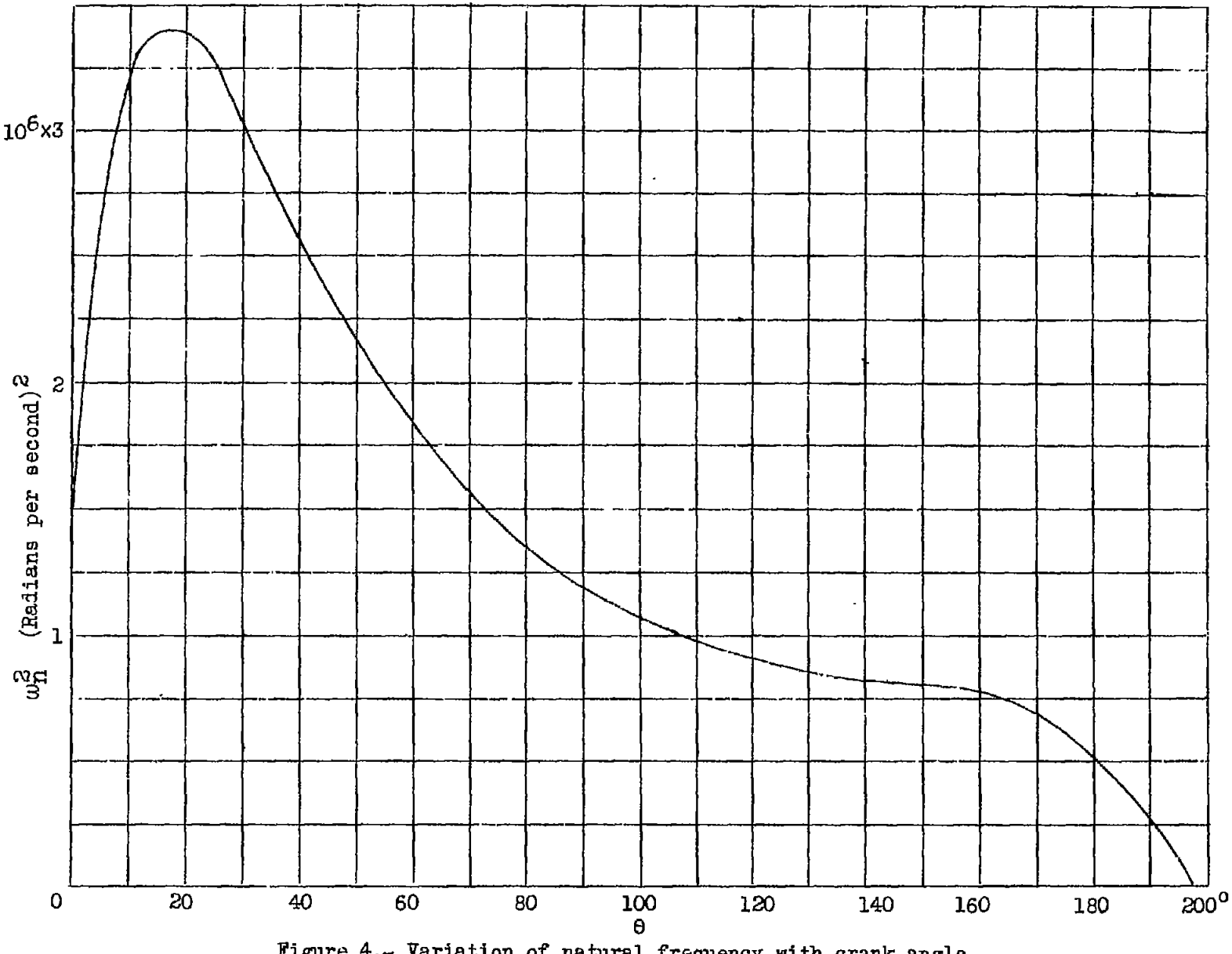

Figure 4.- Variation of natural frequency with crank angle.

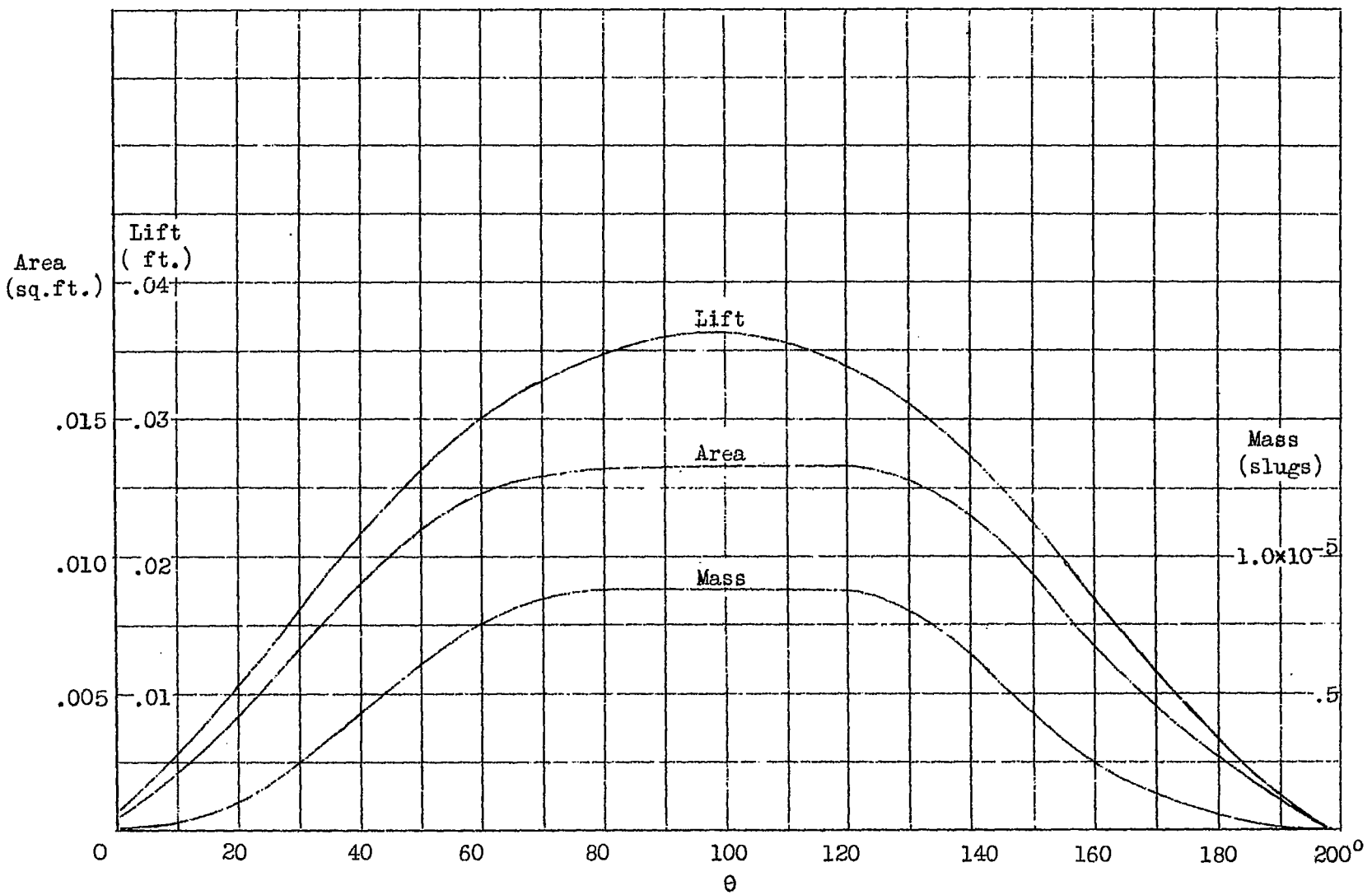

Figure 5.- Variation of valve lift, effective valve area, and effective mass, with crank angle.

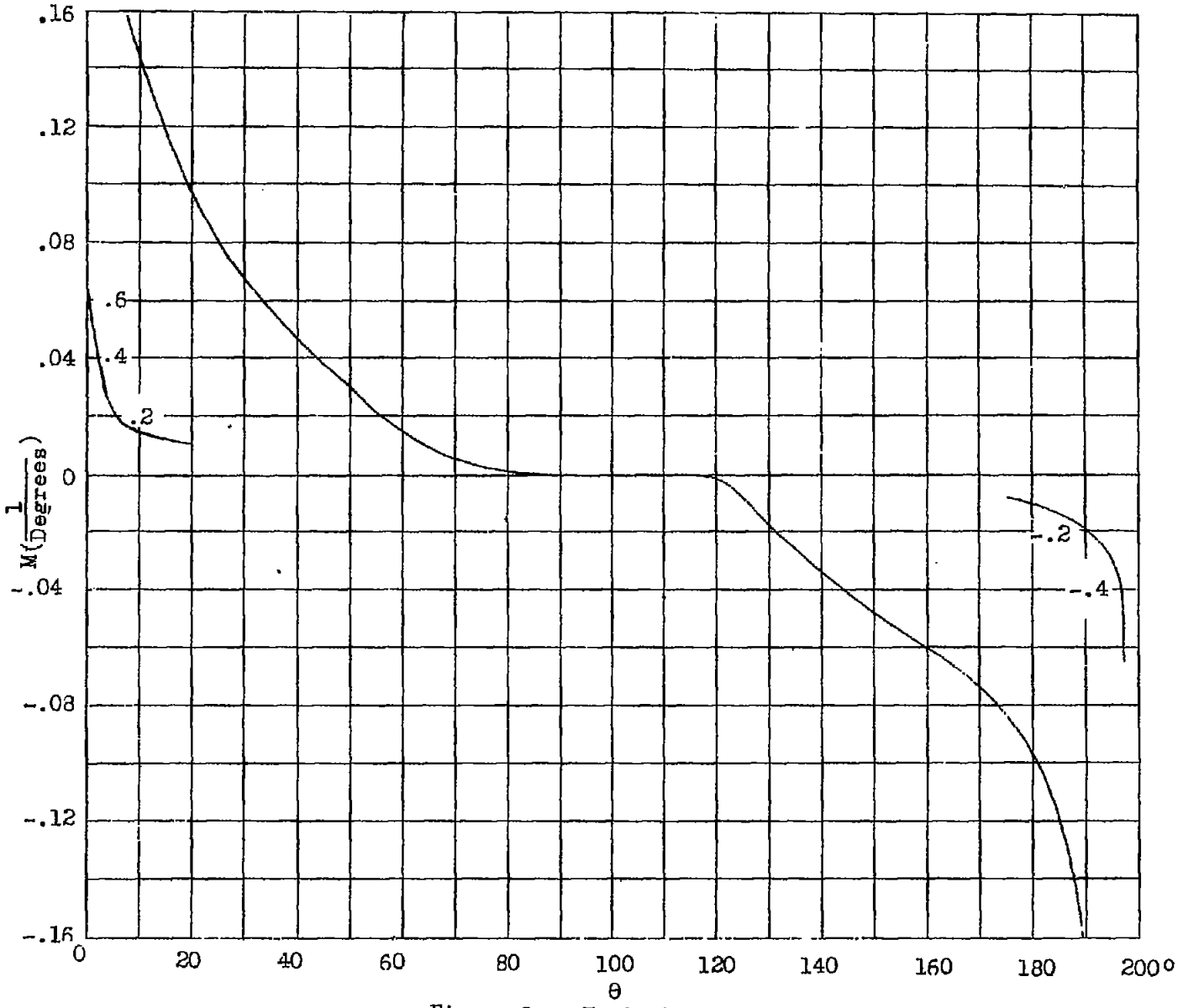

Figure 6.- Variation of M with crank angle.

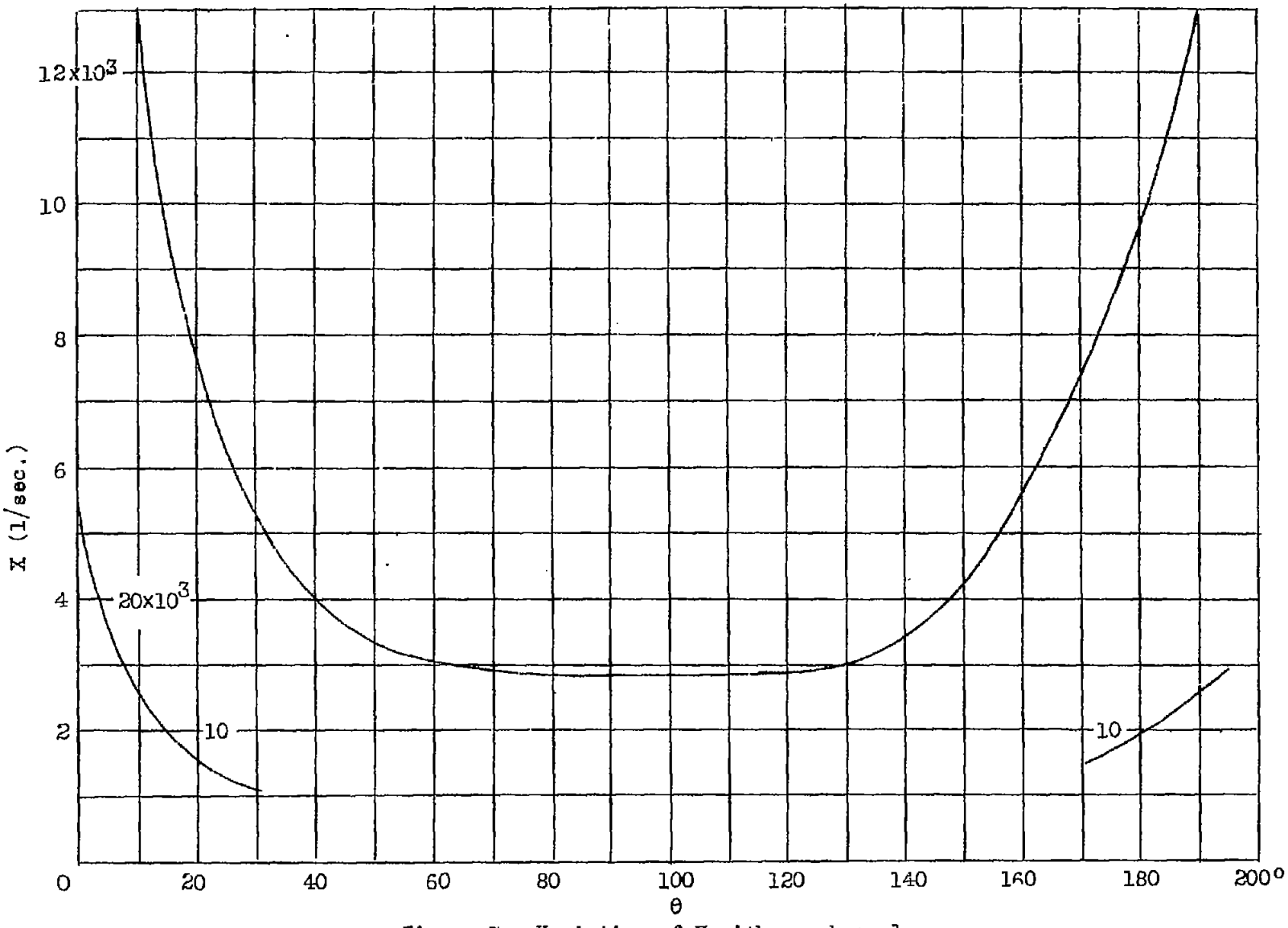

Figure 7.- Variation of X with crank angle.

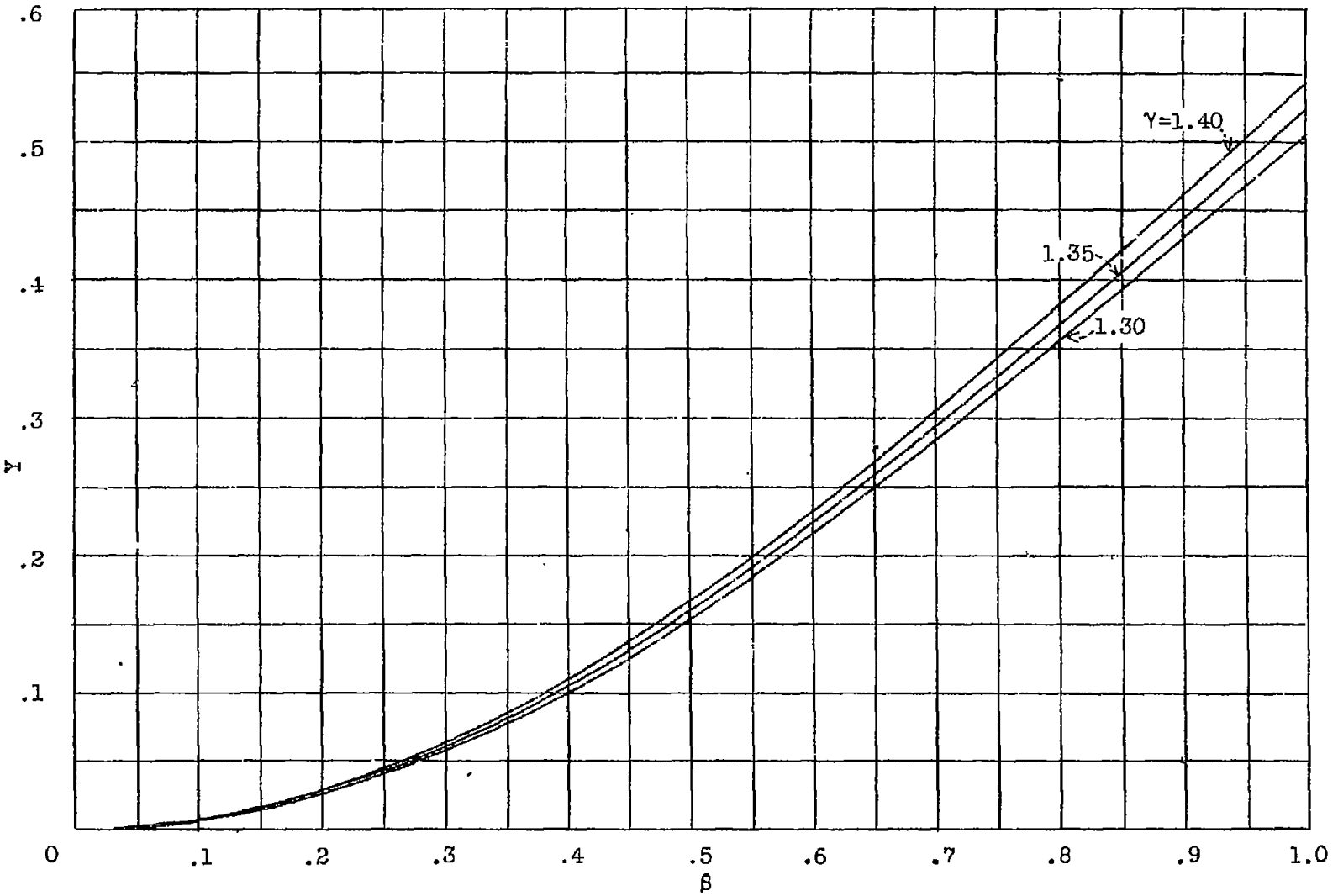

Figure 8.- Variation of Y with β.

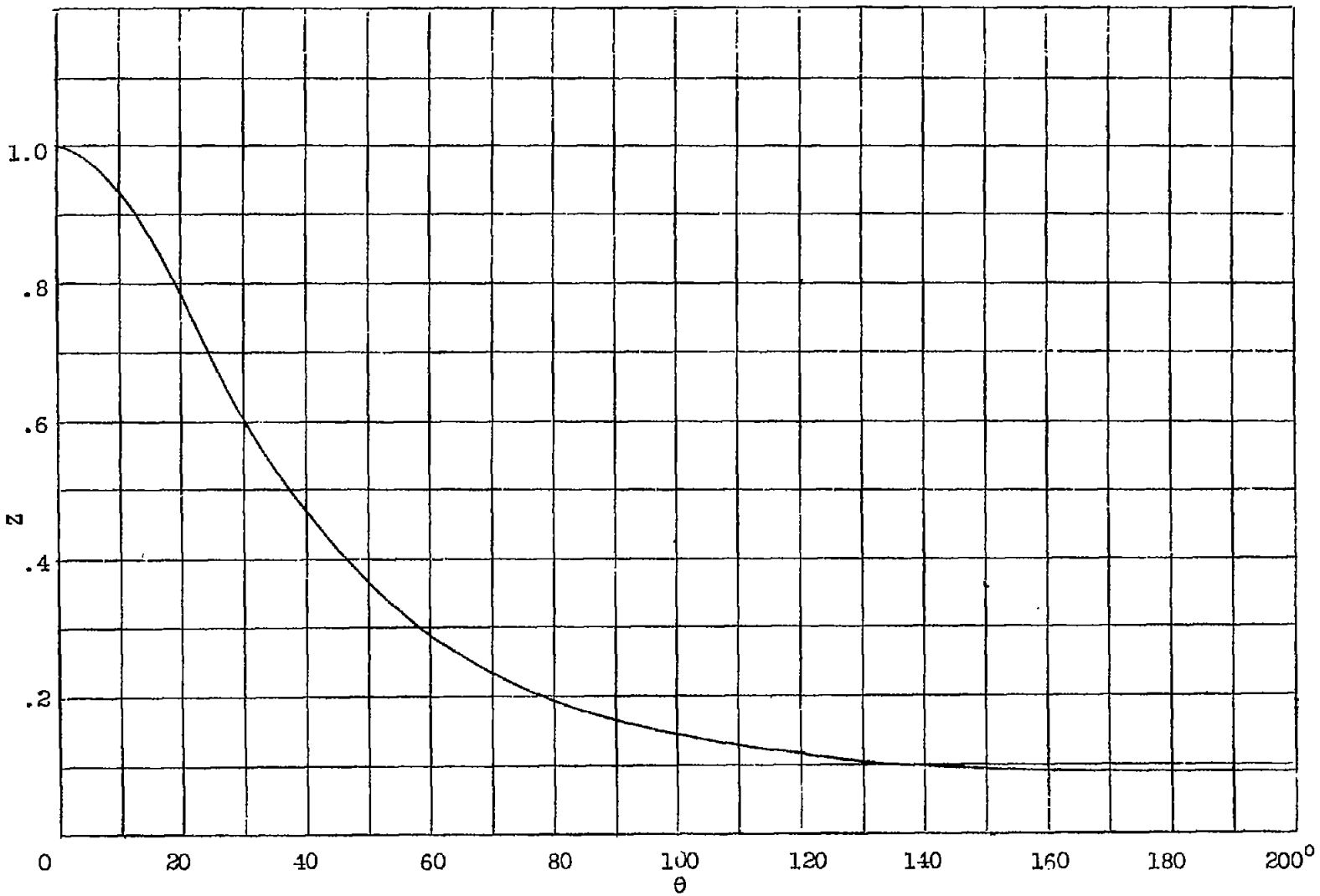

Figure 9.- Variation of Z with crank angle. (γ = 1.3)

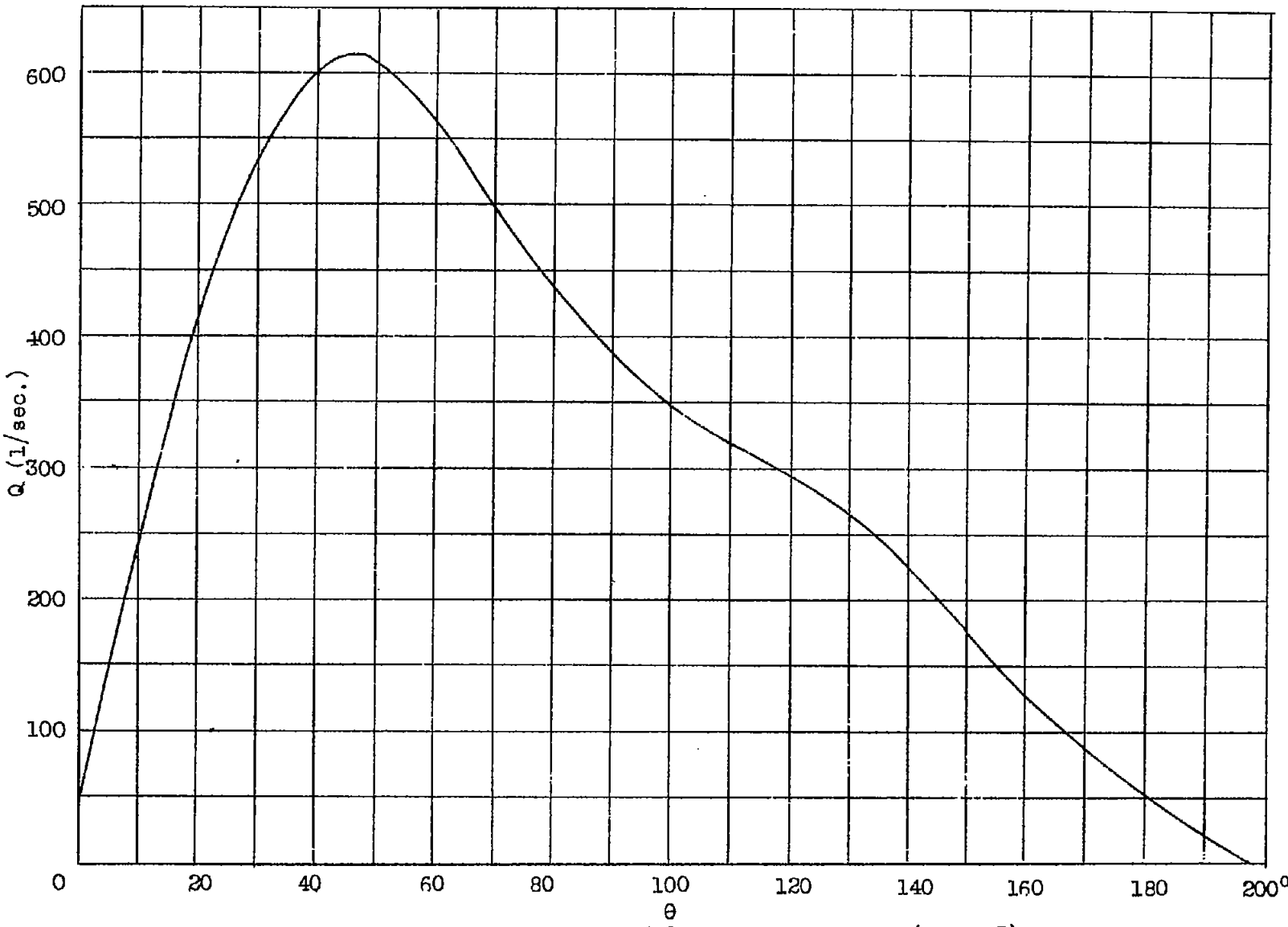

Figure 10.- Variation of Q with crank angle. (γ = 1.3)

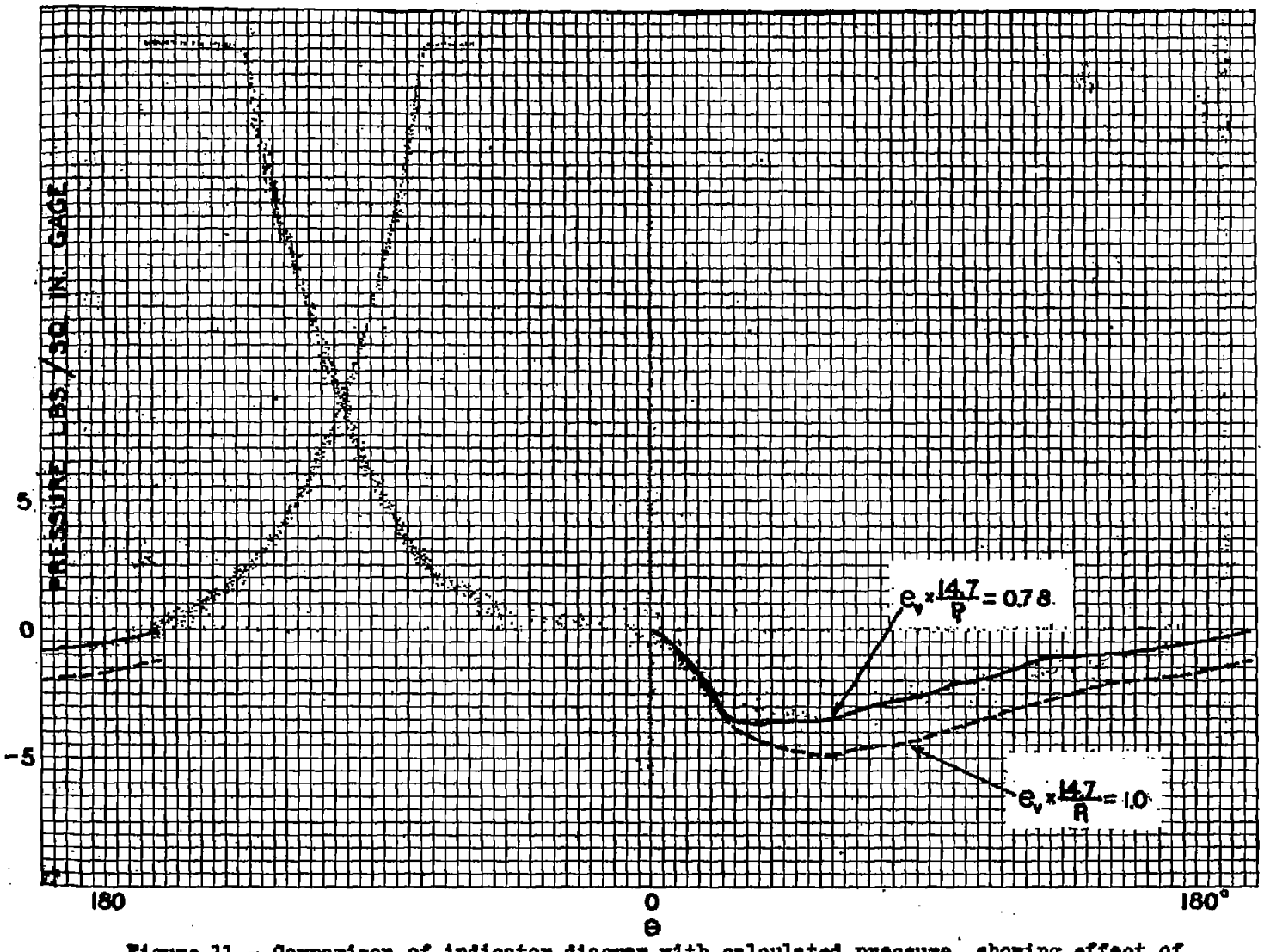

Figure 11.- Comparison of indicator diagram with calculated pressure, showing effect of correcting analysis for thermal effects. 2600 r.p.m.

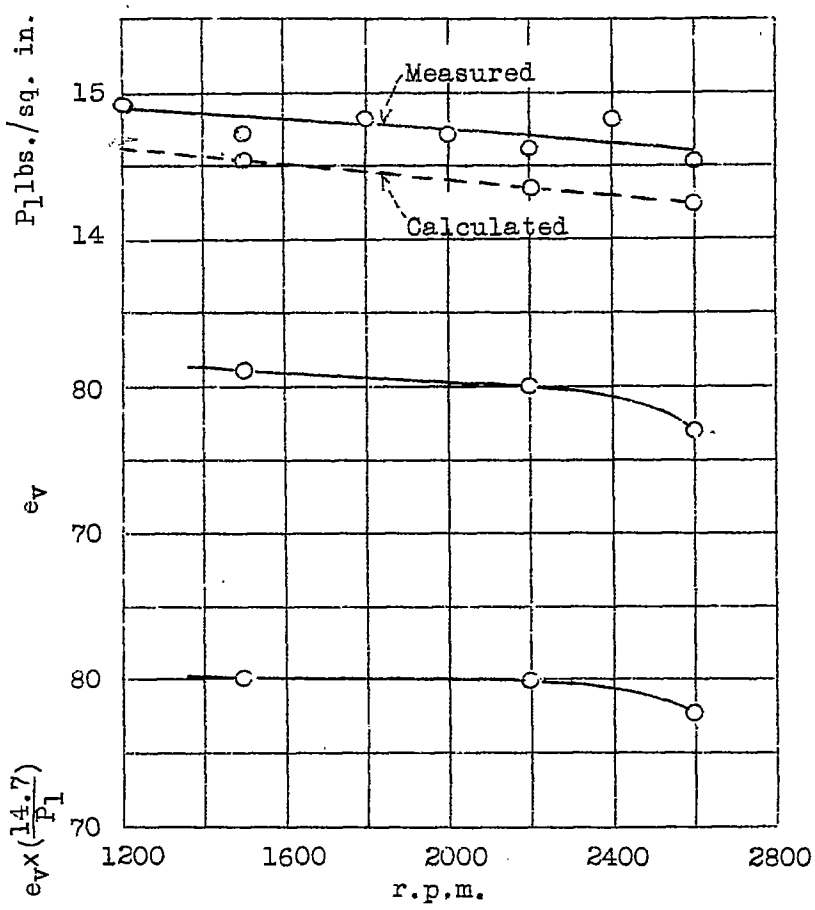

Figure 12.- Variation of P_1 and e_v with r.p.m.

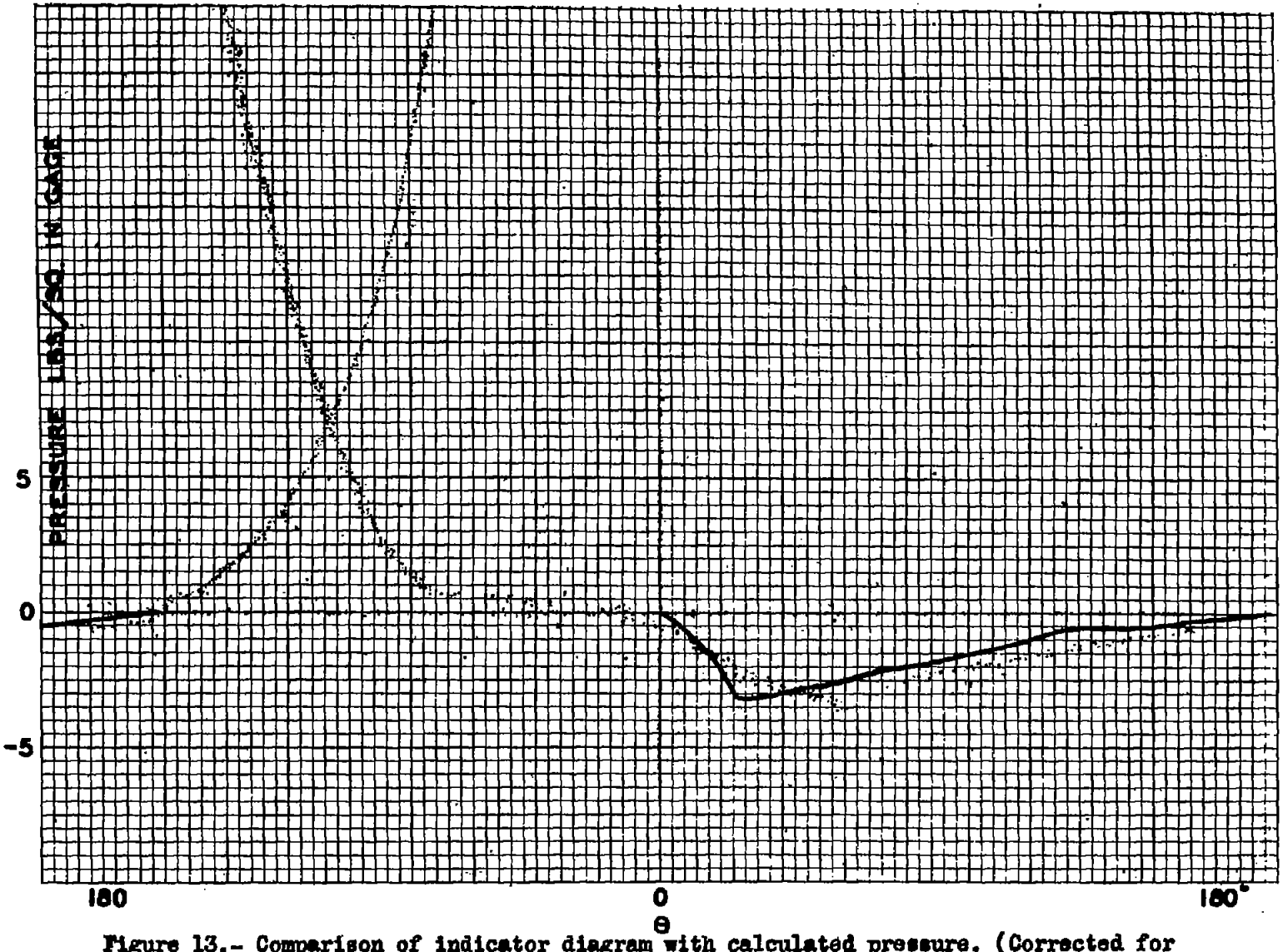

Figure 13.- Comparison of indicator diagram with calculated pressure. (Corrected for $14.7e_v/P_1 = 0.80$.) 2200 r.p.m.

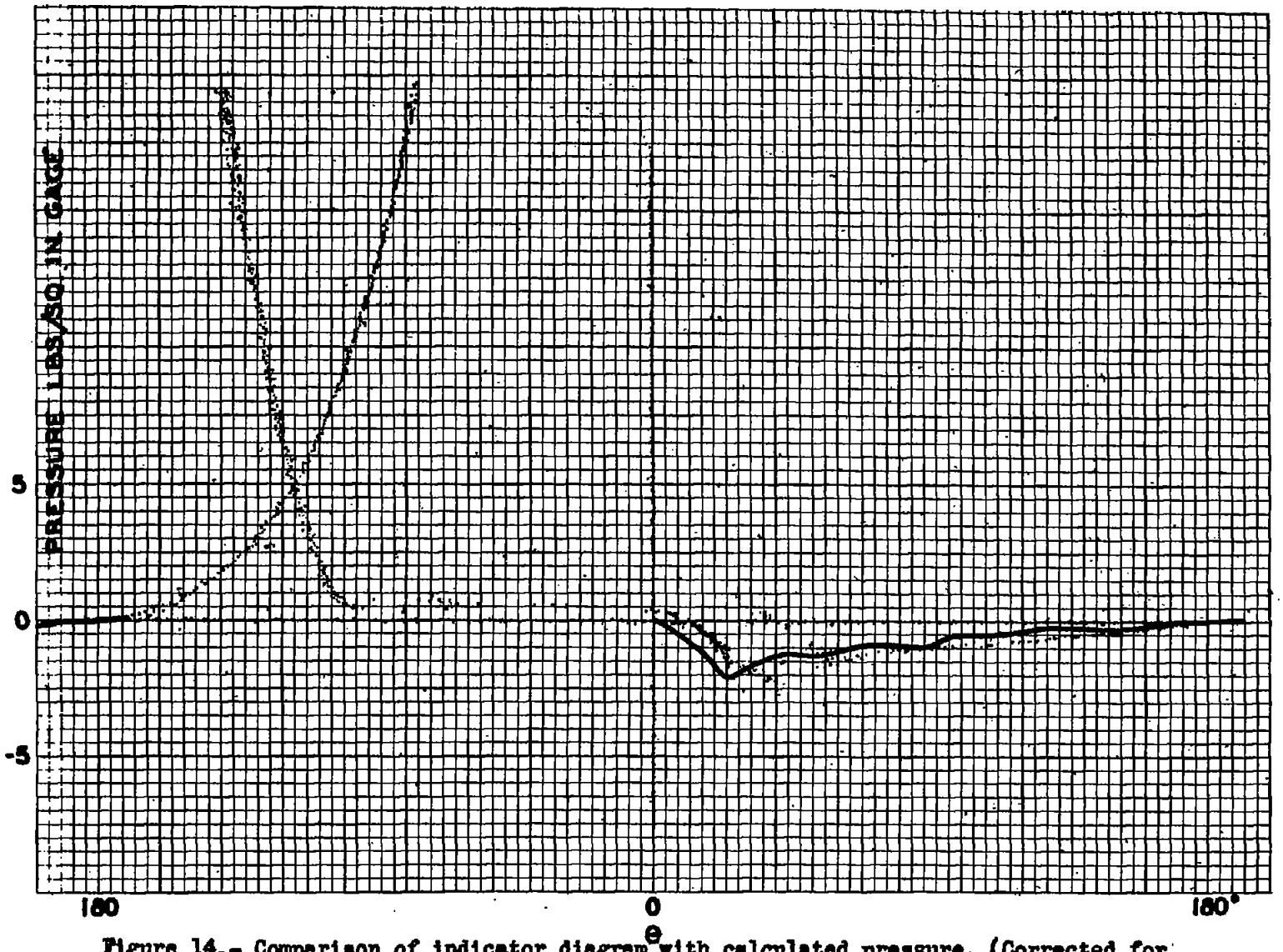

Figure 14.- Comparison of indicator diagram with calculated pressure. (Corrected for $14.7e_v/P_1 = 0.81$.) 1500 r.p.m.

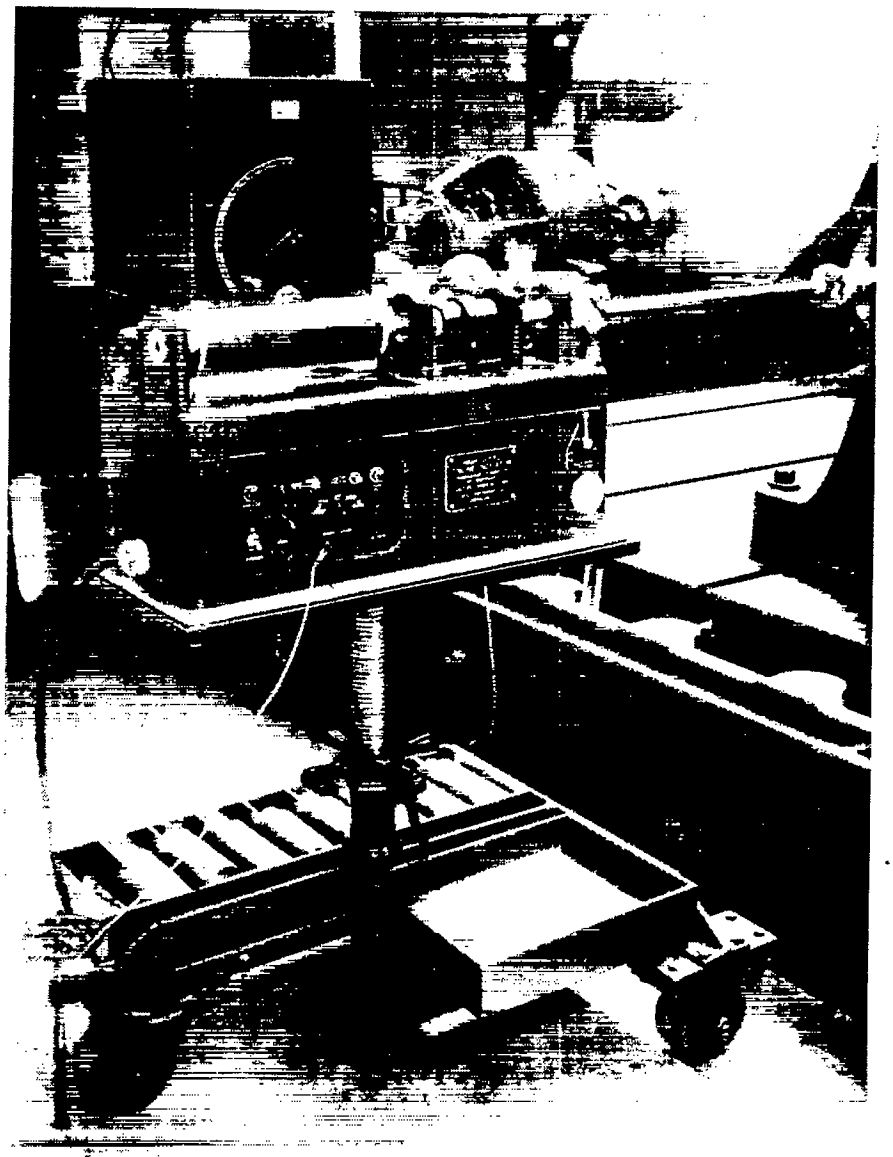

FIGURE 16.-M.I.T. BALANCED PRESSURE INDICATOR

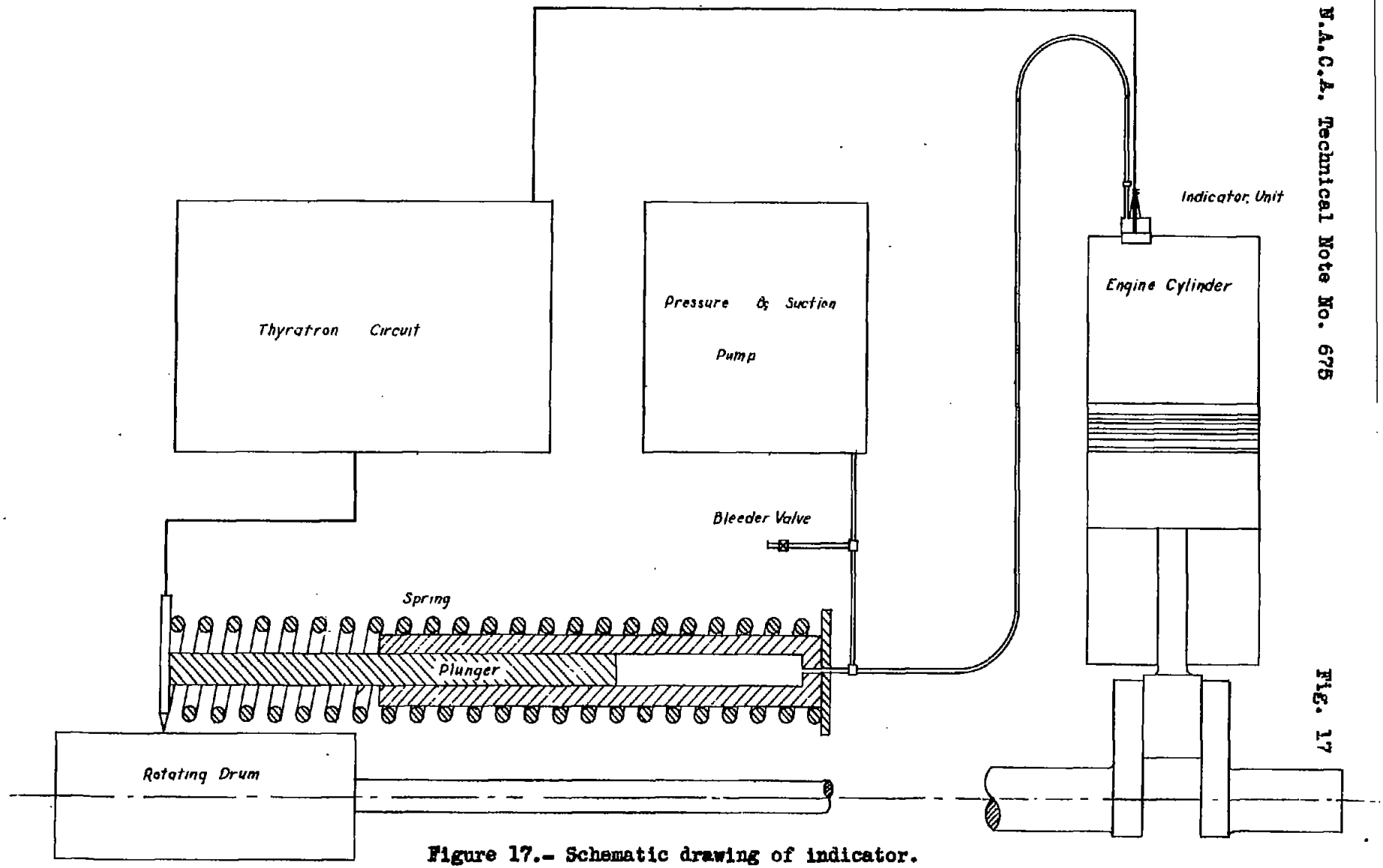

Figure 17.- Schematic drawing of indicator.

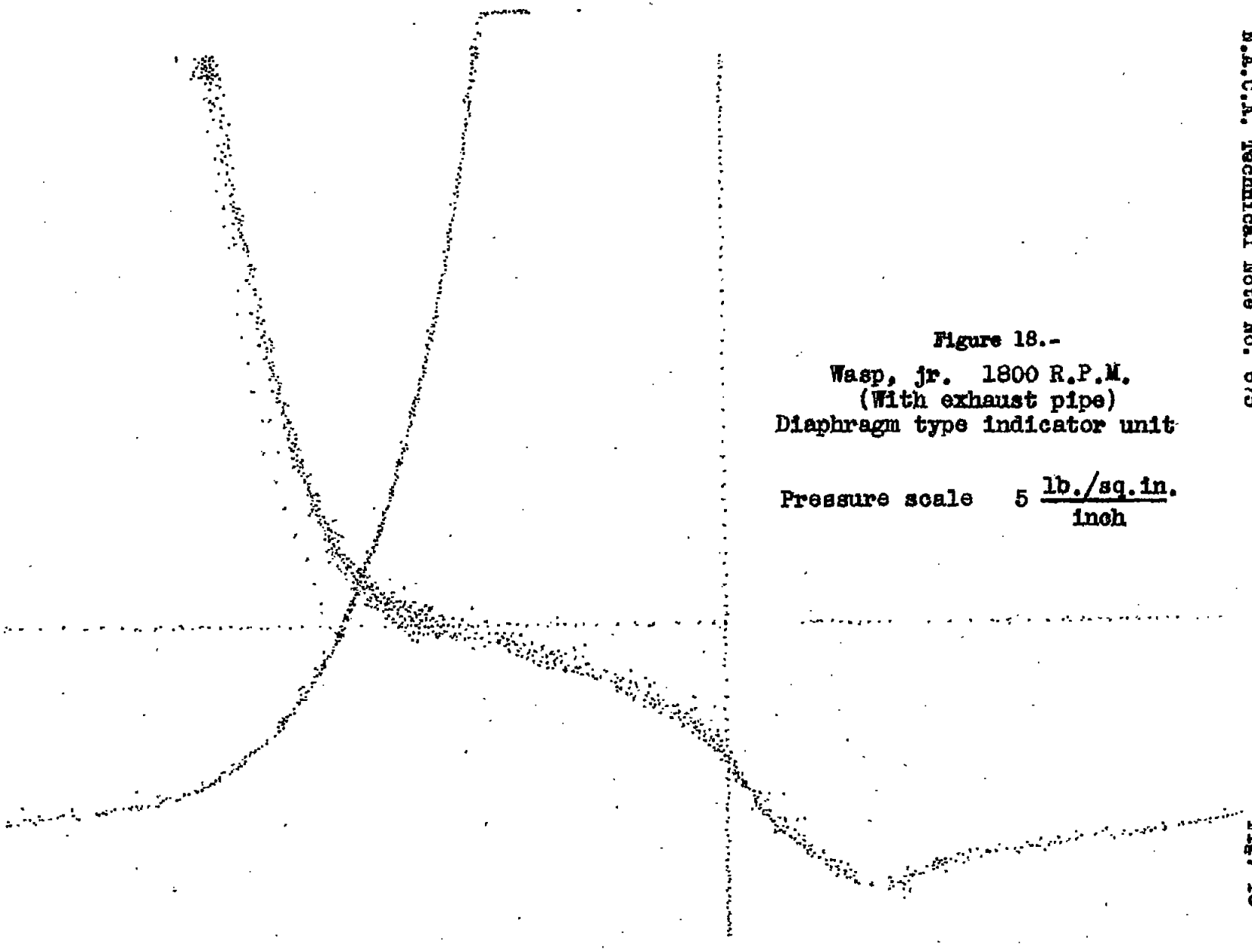

Figure 18.-

Wasp, jr. 1800 R.P.M.
(With exhaust pipe)
Diaphragm type indicator unit

Pressure scale $5 \frac{\text{lb./sq.in.}}{\text{inch}}$

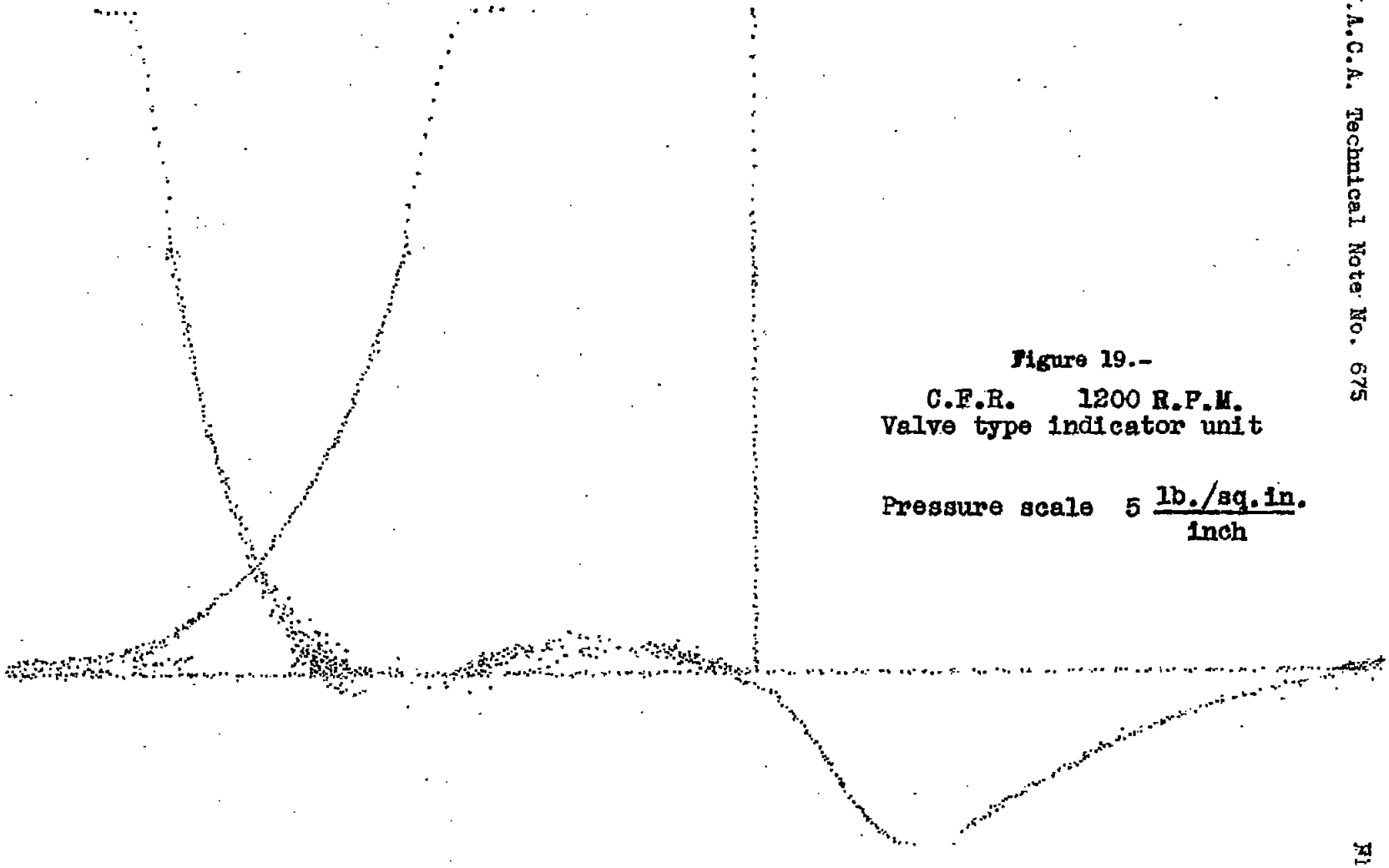

Figure 19.-

C.F.R. 1200 R.P.M.
Valve type indicator unit

Pressure scale 5 $\frac{\text{lb./sq.in.}}{\text{inch}}$

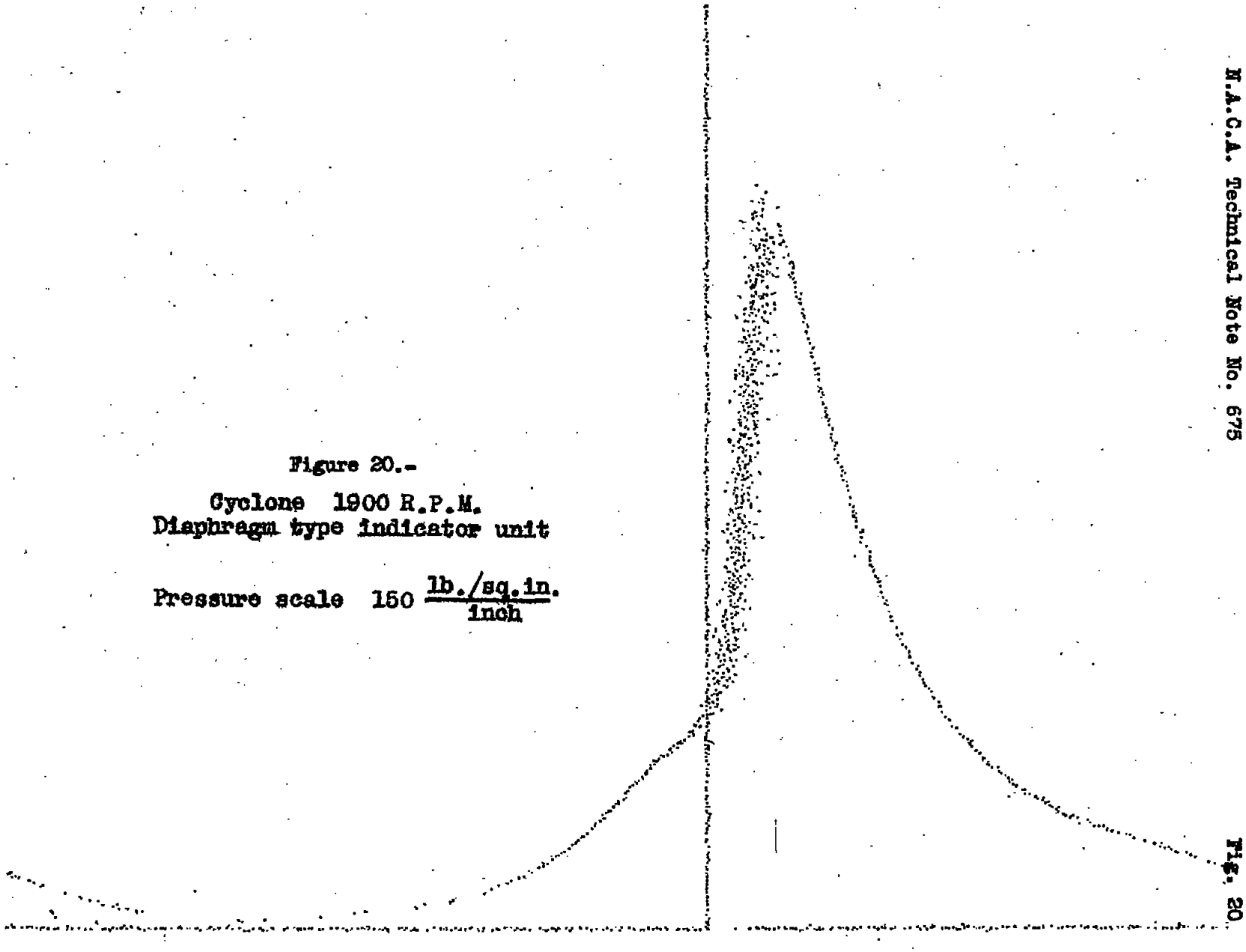

Figure 20.-

Cyclone 1900 R.P.M.
Diaphragm type indicator unit

Pressure scale 150 $\frac{\text{lb./sq.in.}}{\text{inch}}$

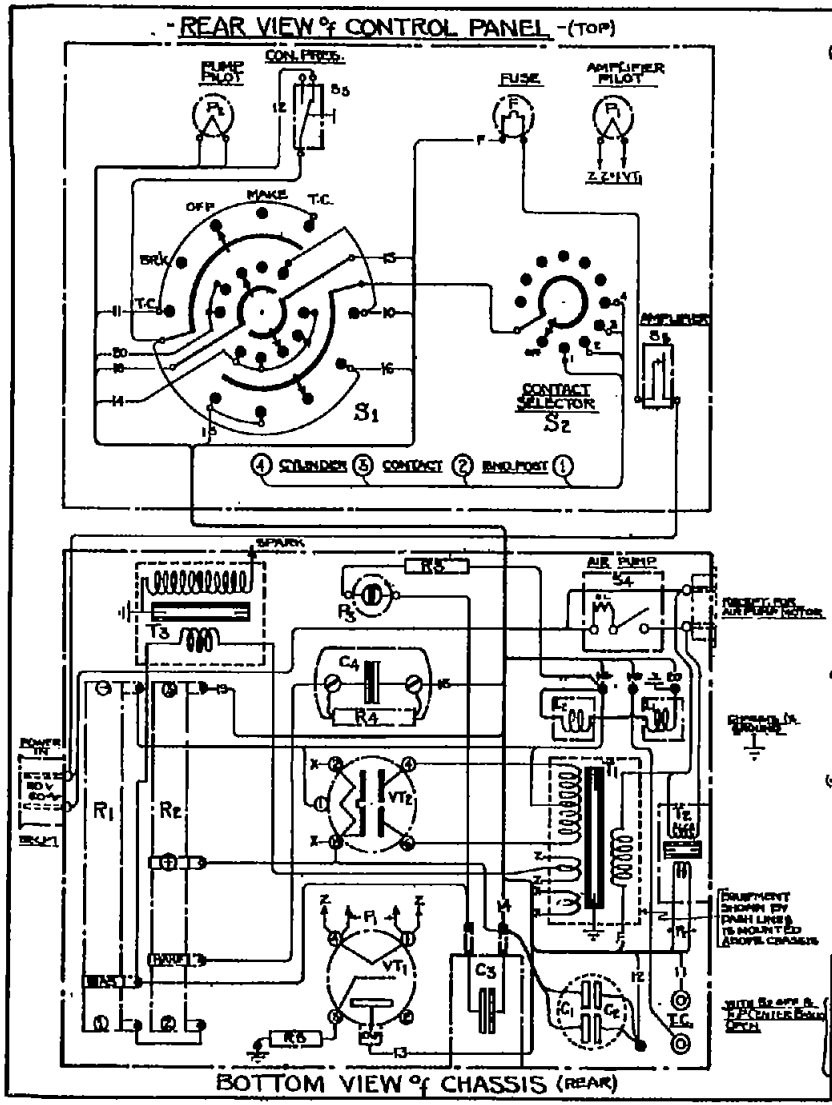

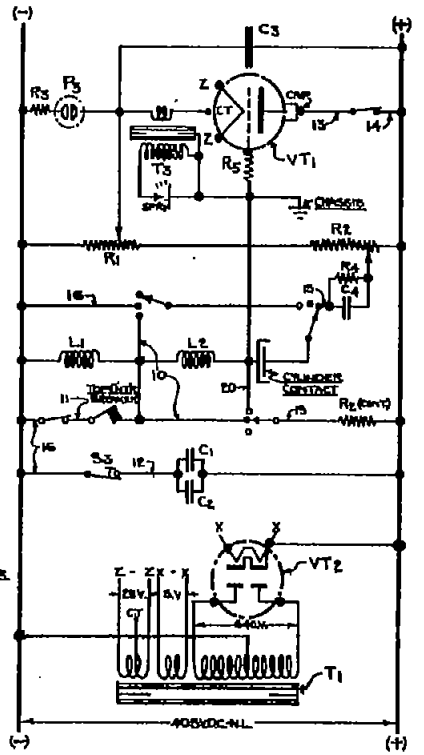

- ELEMENTARY WIRING DIAGRAM -

CONNECTIONS SHOWN SET UP FOR "MAKE" & TOP CENTER OPERATION.
SEE "REAR VIEW OF CONTROL PANEL" FOR CONNECTIONS OF NUMBERED WIRES SHOWN ABOVE TO PANEL SWITCH S1.

- TEST VOLTAGES - WITH METER 1000 Ω/VOLT

- TEST POINTS -		VOLTS - S1 IN POS. BELOW				
	FROM → TO	T.C.	MAKE	OFF	BRKG	T.C.
D.C. POWER	⊖ → ⊕	380	405	405	380	380
"MAKE" CIR.	⊖ → MAKE	140	150	150	140	140
	⊖ → BIAS	34	36	36	34	34
ACTUAL FGHT	⏚ → BIAS	27	36	36	24	24

- LEGEND -

C_{1-2}	CONDENSER - 8-8. μf - 600. WORK.V.
C_3	" - 0.25 μf - 1000. "
C_4	" - 0.012 μf - 1000. "
L_1	INDUCTANCE - 350. M.H. - AIR CORE
L_2	" - " - " "
R_1	RESISTOR - 4000. OHMS - 50. WATT
R_2	" - 75. M. " - 50. "
R_3	" - 20. M. " - 1. "
R_4	" - 250. M. " - 1. "
R_5	" - 20. M. " - 1. "
S_1	SWITCH - 4 CIRCUIT - 5 POSITION
S_2	" - 1 " - 11 "
S_3	" - P.B. TYPE - NORM. CLOSED
S_4	" - S.P.S.T. - 4-A - 250V. - THEK. O.L.
S_5	" - S.P.S.T. - 10A - 250V - TOGGLE
T_1	TRANSFORMER - POWER SUPPLY
T_2	" - HIGH TENSION
T_3	" - PILOT LT. - 120/2.5 V.
P_1	PILOT LT. - AMPLIFIER - 2.5V. - BAY/N'T. BS.
P_2	" " - AIR PUMP - 2.5V. - " "
P_3	" " - SPK. IND. - 115V. - ¼ W. NEON
F	LITTLEFUSE - 3AG TYPE - 0.75A - 500 V.
VT_1	RECTIFIER - GRID CONTROL - GE FG-17.
VT_2	" - HIGH VAC. - TYPE 5Z4

Figure 21

Wiring diagram
M.I.T. - Otico Indicator

RB/7/12/51

WIRING DIAGRAM
SERIAL No 3.
PT303

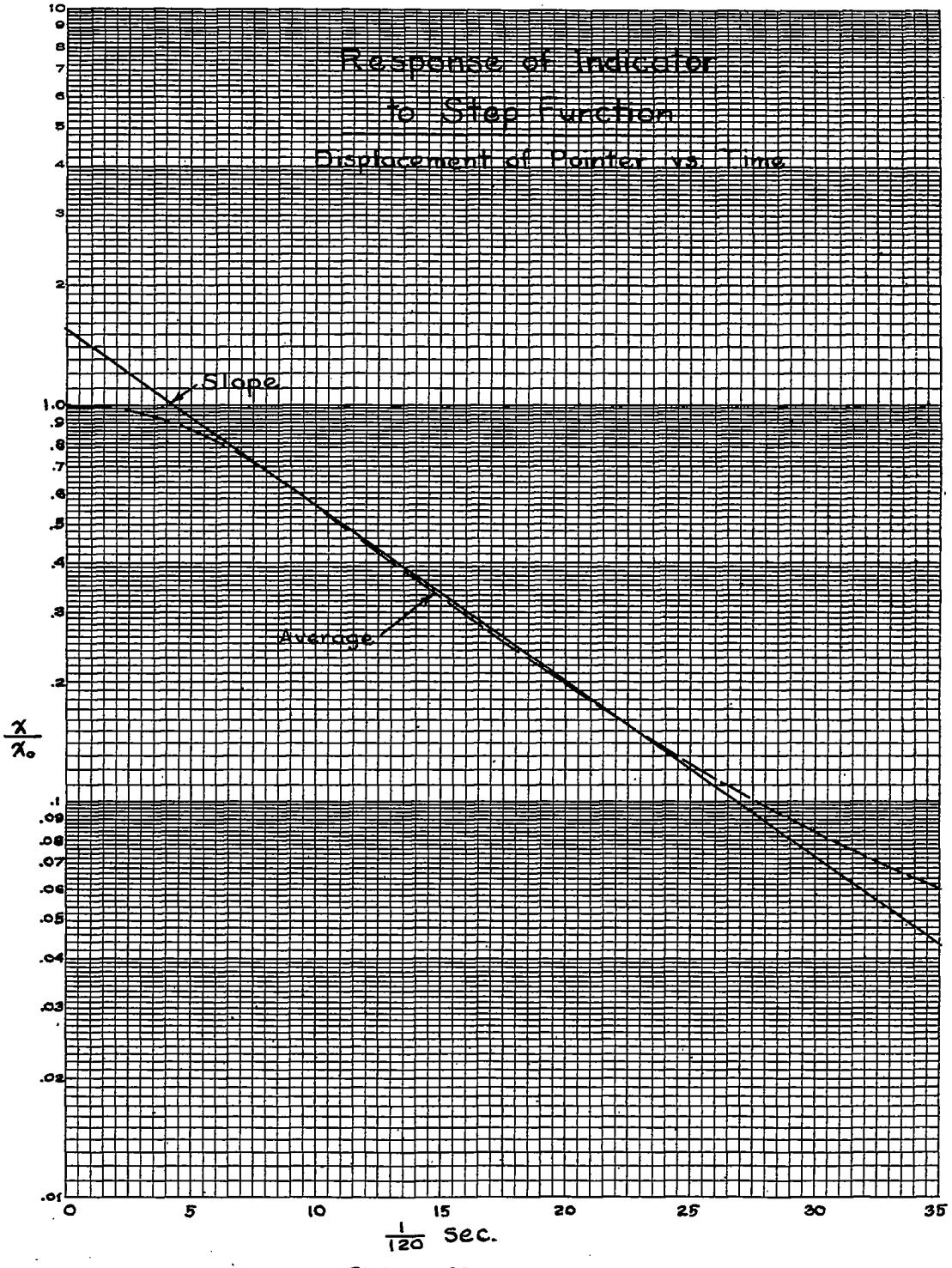
Response of Indicator
to Step Function
Displacement of Pointer vs. Time
Slope
Average
$\frac{x}{x_0}$
10
9
8
7
6
5
4
3
2
1.0
.9
.8
.7
.6
.5
.4
.3
.2
.1
.09
.08
.07
.06
.05
.04
.03
.02
.01
0
5
10
15
20
25
30
35
$\frac{1}{120}$ Sec.

Figure 22

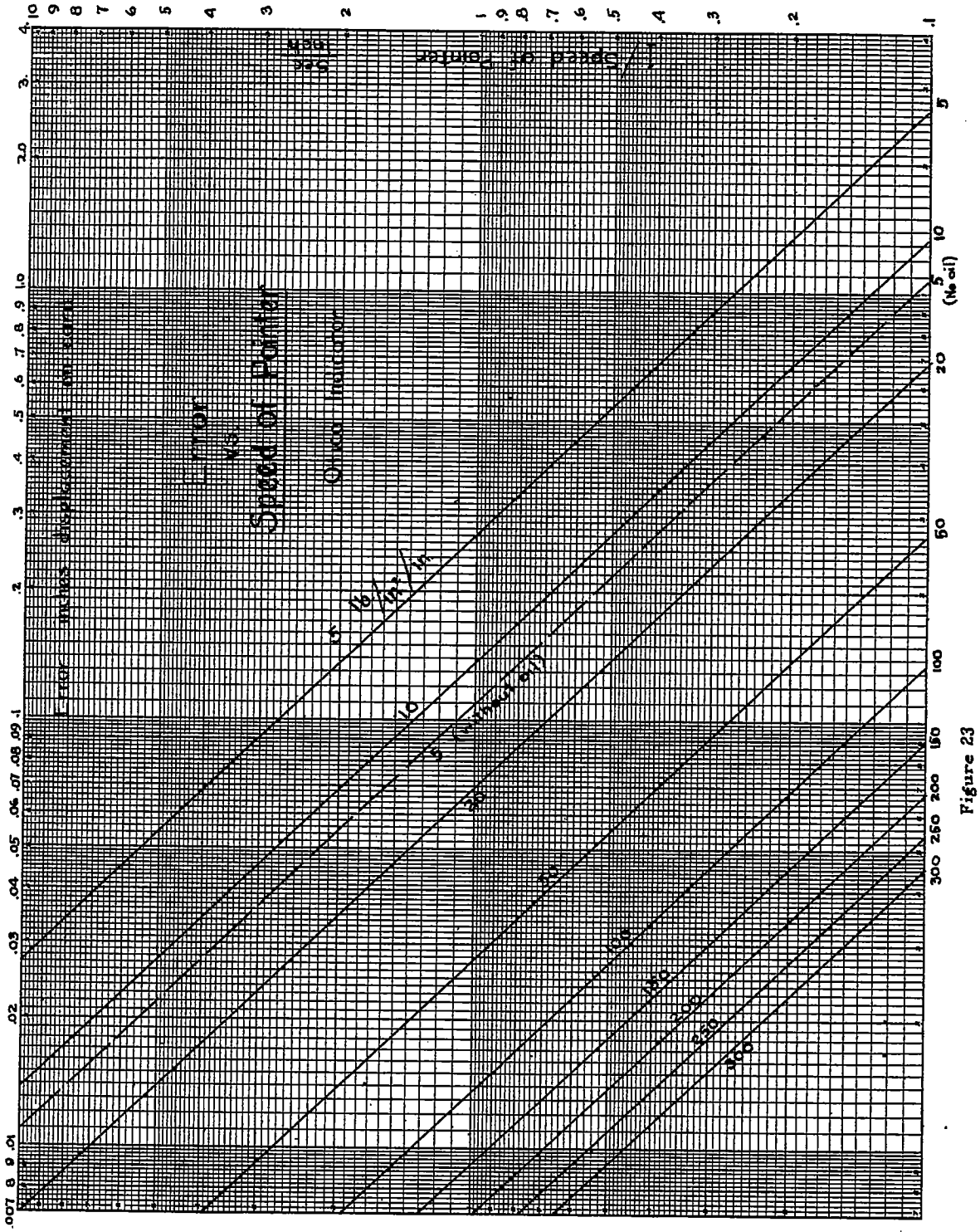
Error vs. Speed of Pointer
Orica Indicator
Error inches displacement on cam
1/Speed of Pointer Sec/inch
5 lb./in²/in.
10
5 (without oil)
20
50
100
150
200
250
300
5 (No oil)
10
20
50
100
150
200
250
300

Figure 23

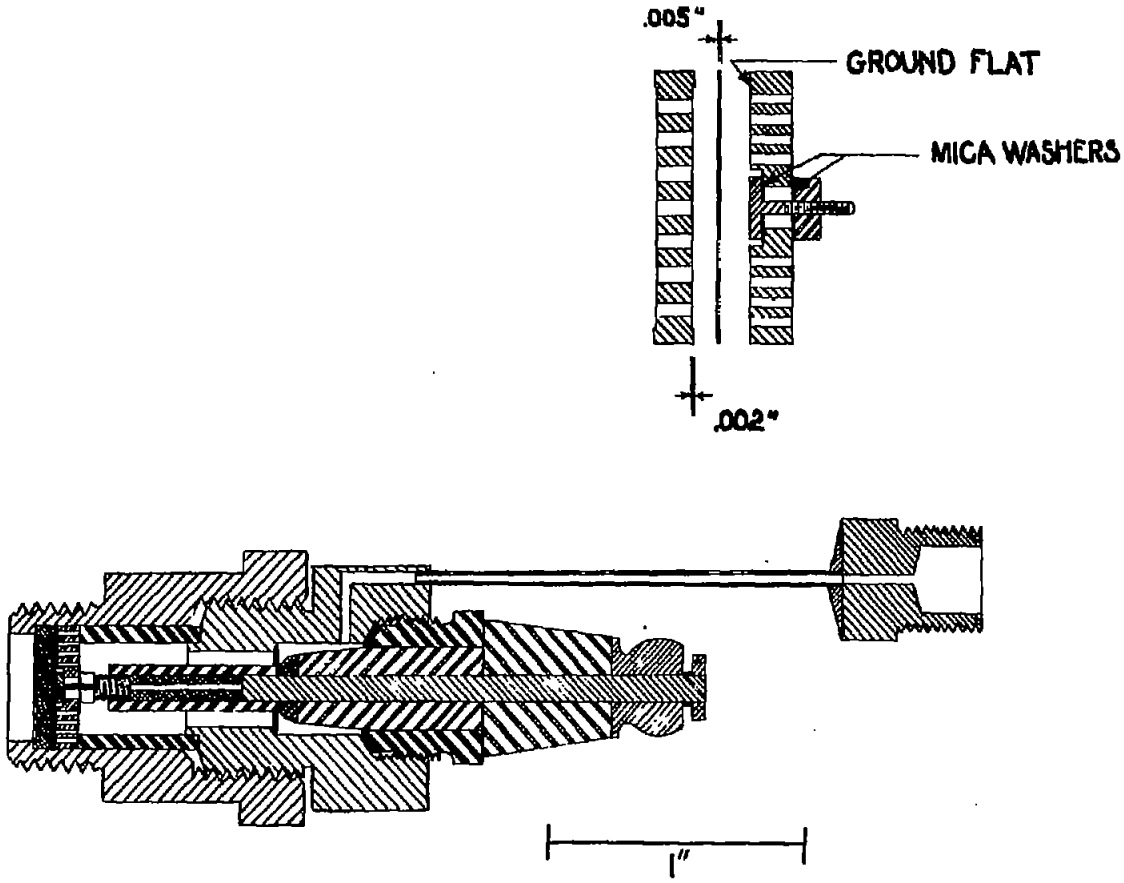

Figure 24.-

DIAPHRAGM INDICATOR UNIT

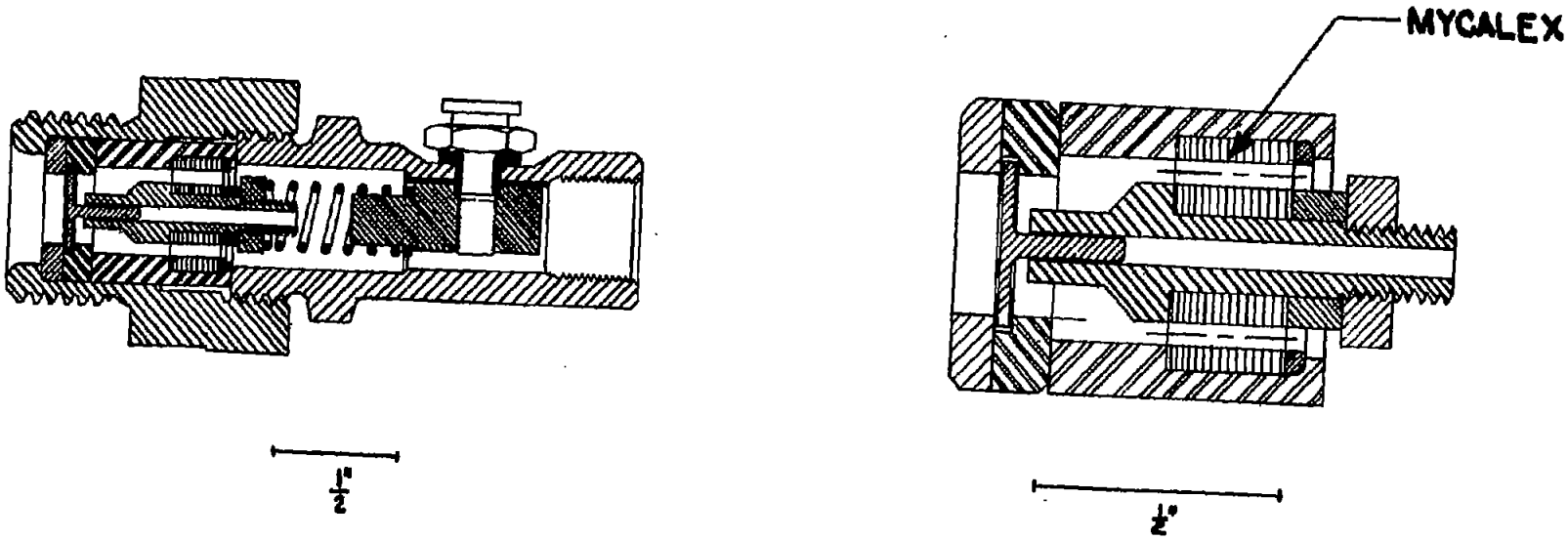

VALVE INDICATOR UNIT

Figure 25.

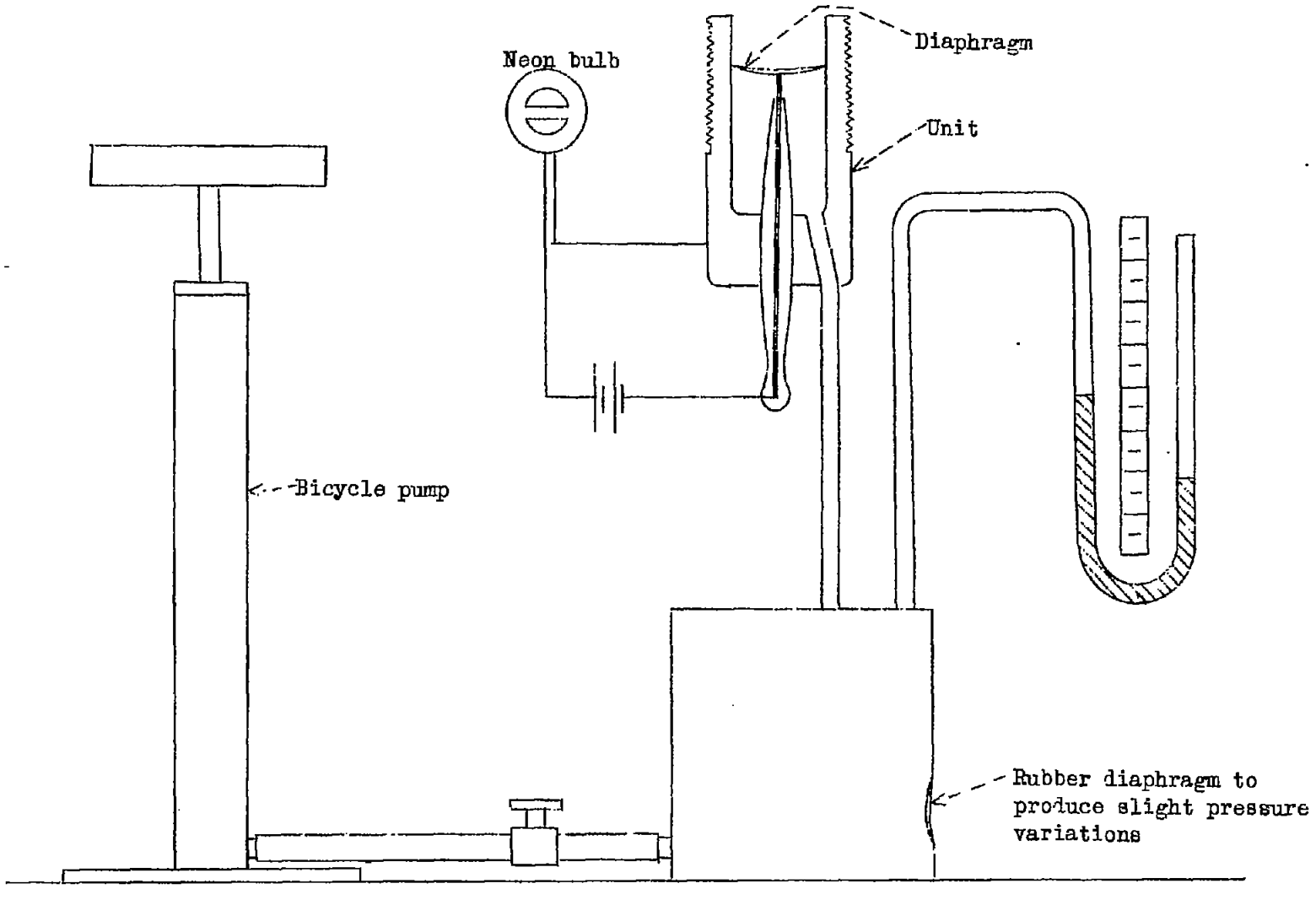

Figure 26.- Static calibrator.

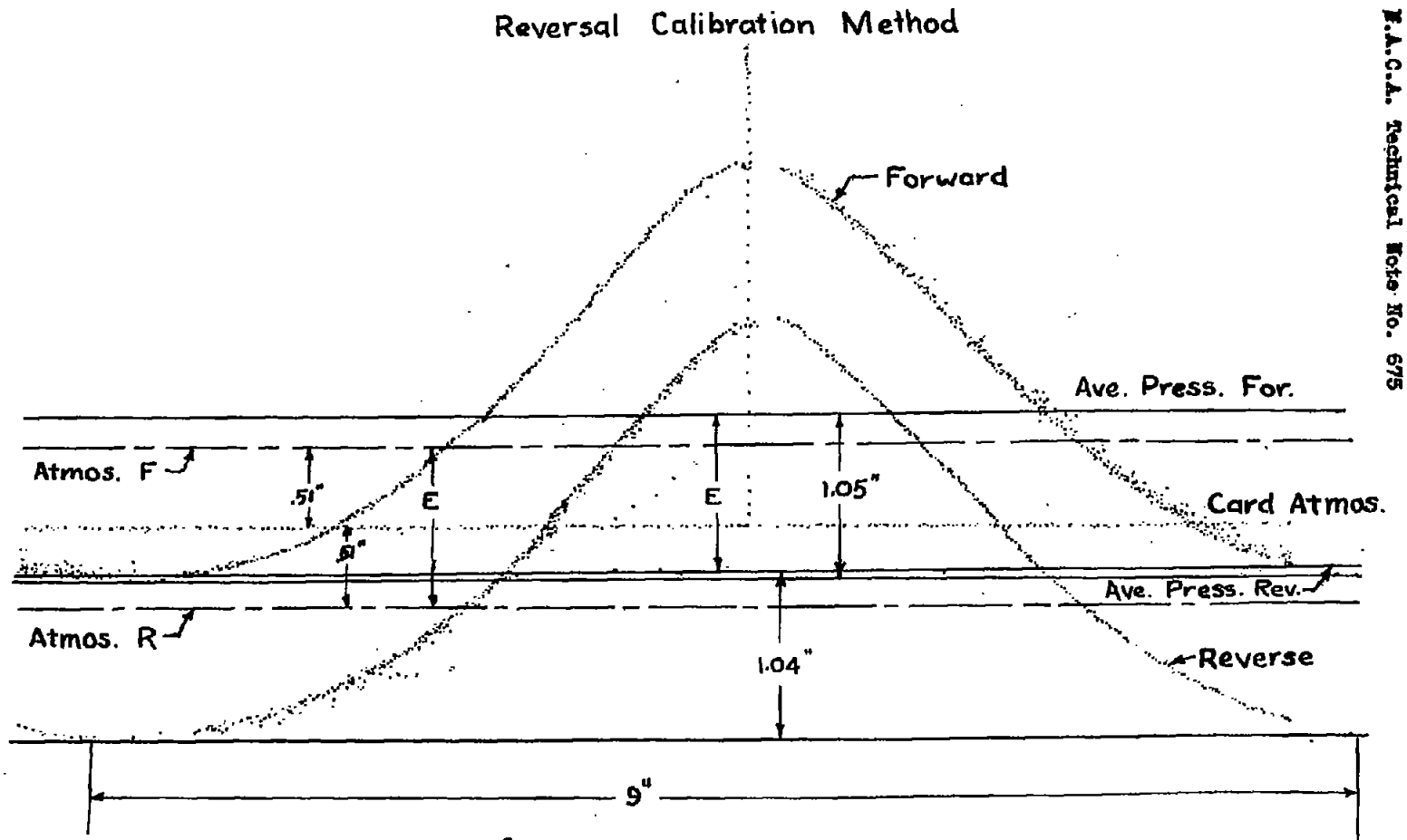

Area Under Forward = 9.45 in.²
Average Pressure = $\frac{\text{Area}}{\text{Length}}$ = 1.05" above base line

Area Under Reverse = 9.40 in.²
Average Pressure = 1.04"

∴ E = 2 × zero error ≐ 1.02"

Press. Scale – 5 lb/in.² = 1 in.

Zero Error = $\frac{1.02}{2} \times \frac{5}{.491}$ = 5.2 in. Hg.

Figure 27.